SERI/STR-211-2515
UC Category: 63
DE85008772

Zn_3P_2 as an Improved Semiconductor for Photovoltaic Solar Cells

Final Report
1 April 1983 - 31 March 1984

A Subcontract Report

M. Bhushan
J. D. Meakin
Institute of Energy Conversion
University of Delaware

March 1985

Prepared under Subcontract No. XE-2-02048-1

SERI Technical Monitor: R. Mitchell

Solar Energy Research Institute
A Division of Midwest Research Institute

1617 Cole Boulevard
Golden, Colorado 80401

Prepared for the
U.S. Department of Energy
Contract No. DE-AC02-83CH10093

1. ABSTRACT

Development efforts have been made on two heterojunctions with Zn_3P_2 namely Zn_3P_2/ZnSe and Zn_3P_2/(CdZn)S. In both cases improved open circuit voltages were achieved but control of the material properties of the heterojunction partner has limited short circuit currents and overall efficiency. In the case of ZnSe, the high resistivities of deposited thin-films were efficiency limiting on all devices. In the case of (CdZn)S, it is concluded that high interface recombination rates are controlling the short circuit current and limiting the overall efficiency. A more fundamental study of the Zn_3P_2/(CdZn)S heterojunction will be necessary in order to make further optimization of this device possible.

2. TABLE OF CONTENTS

		Page
1.	ABSTRACT	ii
2.	TABLE OF CONTENTS	iii
3.	INTRODUCTION	1
4.	Zn_3P_2/ZnSe HETEROJUNCTION DEVICES	4
5.	Zn_3P_2/(CdZn)S HETEROJUNCTION DEVICES	21
6.	FUTURE RESEARCH	49
7.	REFERENCES	51
	APPENDIX	

3. Introduction

In 1976, the United States Energy Research & Development Administration issued a request for proposals to develop improved semiconductors for photovoltaic solar cells. As a result of that RFP, a number of programs were initiated but only one addressed an essentially new compound semiconductor for photovoltaics. That semiconductor, Zn_3P_2, is comprised of elements that are essentially in unlimited supply, has a bandgap close to the commonly accepted optimum for a single junction solar cell and is a direct bandgap strongly absorbing material. Furthermore, it has been shown that although presently limited to p type conductivity, the electron mobility and lifetime is excellent yielding diffusion distances of the order of 10 μm.

From 1976 until the end of the present contract a cell development program has been maintained continuously at the Institute of Energy Conversion. The Appendix gives the relevant contract numbers, sponsoring agency and periods of performance. Although during the first year or two of the IEC program, some fundamental studies of the preparation and basic properties of Zn_3P_2 were, for most of that time, carried out, development of high efficiency solar cells has been emphasized. In contrast to such materials as GaAs, there has not been extensive interest in Zn_3P_2 outside of potential photovoltaic use and accordingly there has not been the development of a broad basic body of information on Zn_3P_2.

In common with a number of other embryonic solar cell programs, initial efforts were directed to developing Schottky devices which in the case of Zn_3P_2 met with a considerable degree of success. However, it was realized that a Schottky device was unlikely to provide the basis of a commercial solar cell and accordingly for the last few years, attention has been focussed on

developing a high efficiency heterojunction.

With a p type absorber, the optimum heterojuction partner would be a wide gap n type semiconductor to act both as a window and the origin of a charge separating junction. The number of materials with an appropriate bandgap is small and the choice is further reduced by the requirement that the electron affinity match that of Zn_3P_2. During part of the present contract period, attention was focussed on developing a Zn_3P_2/ZnSe heterojunction. ZnSe most certainly has an appropriate bandgap but thin films generally have a high resistivity and this ultimately proved to be an insurmountable obstacle to production of an efficient cell. The latter part of the present year was therefore focussed on (CdZn)S, a material with which IEC has had some substantial experience and success albeit at relatively low Zn concentrations. When the present program was terminated, it was evident that the quality of the interface between Zn_3P_2 and (CdZn)S was efficiency limiting and that a fundamental study of this interface using high resolution imaging and analysis techniques could perhaps direct future development efforts.

The average level of effort under federal sponsorship applied to both the fundamental and applied research aspects of Zn_3P_2 development has been only equivalent to about 3 researchers. Furthermore, except for some crystal growth and alloy work in Poland and an isolated study in Japan, there has been no significant input of research results from any other source. In spite of this the research at IEC has made some substantial basic and applied contributions to the understanding and potential application of Zn_3P_2.

Good quality Zn_3P_2 single crystals have been grown and some success in extending the technique to Cd_3P_2-Zn_3P_2 alloys was achieved. The origin of the normal charge carriers, namely holes, was identified conclusively and

techniques for both intrinsic and extrinsic control of carrier density developed. Fundamental optical measurements have been made and reported. Large grain size thin-films were deposited on a stable ohmic contact developed at IEC.

As a consequence of the various device development programs carried out, a contribution to the understanding of Schottky barrier heights was made with a semiconductor other than Si or the extensively studied III-V materials.

Schottky barrier grid devices with total area efficiencies of over 6% and an active area efficiency of 7.6% were produced. The naturally occurring surface and grain boundaries in Zn_3P_2 were both shown to have low recombination velocities without any special treatments. A homojunction was created by in-diffusion of Mg but the measured diffusion coefficient was shown to be too high at room temperature to yield a useable homojunction. Active heterojunctions were made with ZnO, CdS, (CdZn)S and ZnSe.

A complete listing of IEC reports and published papers is given in the Appendix.

4. Zn_3P_2/ZnSe Heterojunction Devices

Extensive attempts were made to produce low resistivity ZnSe thin-films for use in a Zn_3P_2/ZnSe heterojunction. It was found possible to produce an acceptable resistivity ZnSe when the film was deposited on selected substrates. However, these substrates in general preclude the production of a Zn_3P_2/ZnSe backwall heterojunction and in some cases degradation of the carrier properties of Zn_3P_2 were observed presumably due to deleterious interaction with the substrate material.

4.1 ZnSe Thin-Film Deposition

Ga or Al doped ZnSe films were deposited by co-evaporating ZnSe powder and Ga/Al in vacuum. The source materials were placed in boron nitride bottles which were 7.5 cm in length, had an inner diameter of 1 cm and were heated with a two zone heater. Chromel-alumel thermocouples were inserted in the top and bottom parts and the temperatures were maintained at the desired set-points. The top of the source bottle was always kept at a temperature higher than the bottom to prevent any material from condensing there. The substrate holder consisted of a frame capable of holding nine 1" x 1" substrates. It was heated radiatively and the substrate temperature, measured by attaching a thermocouple to a 7059 glass slide placed in the substrate holder, could be varied between 150-450°C. The ZnSe and Ga/Al source bottles were placed a few cms apart and tilted to ensure uniform mixing of the vapor. The source-to-substrate distance was 15 cm.

In earlier experiments[1], Ga doped ZnSe films were deposited on ITO coated 7059 glass substrates. ZnSe/Zn_3P_2 devices were prepared by growing a Zn_3P_2 film on ZnSe by close-spaced vapor transport (CSVT). It was found that if the Ga concentration in the film was > 0.5%, Ga_2Se_3 precipitation took place during processing and the device characteristics were not rectifying. For device applications, the Ga source temperature was adjusted to give a Ga concentration of < 0.2% in the ZnSe film.

Similar experiments were conducted with Al as a dopant in ZnSe. ZnSe/Zn_3P_2 devices were prepared on glass/ITO substrates and the cell performance was used to determine the level of doping acceptable for device applications. The Al concentration in the film was estimated from the effusion rates and is given by the following equation

$$\frac{N_A}{N_Z} = \frac{\alpha_A P_A S_A \beta_A}{\alpha_Z P_Z S_Z \beta_Z} \left(\frac{T_Z M_Z}{T_A M_A}\right)^{1/2} \quad (1)$$

where α is the evaporation coefficient, P is the vapor pressure at the source temperature T, S is the sticking coefficient on the substrate, β is a factor dependent on the geometry of the source bottle and M is the molecular weight. The subscripts A and Z refer to Al and ZnSe respectively.

The ZnSe source and the glass substrates coated with ITO were heated to 1040°C and 260°C respectively and the Al source temperature was varied between 990°C and 1120°C. The ratio N_A/N_Z under these conditions was ~ 0.0002. Zn_3P_2 films were deposited on ZnSe by CSVT and ohmic contact to Zn_3P_2 was made with an evaporated film of Au. ITO served as a transparent back contact to ZnSe. The cell characteristics were comparable to similar devices with Ga doped films ($V_{oc} \sim 0.5$ Volt, $J_{sc} \sim 0.2$ mA/cm^2). There was no correlation between the cell parameters and the Al concentration. The film resistivity was $> 10^4$ Ω-cm. When the Al source temperature was raised to 1220°C $N_A/N_Z = 0.02$, the films turned orange in color and did not adhere well to the glass substrate.

The film resistivity remained high ($> 10^4$ Ω-cm) even at high doping levels ($> 10^{17}$ cm^{-3}). For both Al and Ga doped ZnSe films the Zn_3P_2/ZnSe devices had light generated currents of < 1 mA/cm^2.

4.2 ZnSe Films on Single Crystal Substrates

In all the works published on the various methods of depositing conducting ZnSe films (e.g. vacuum evaporation, organometallic chemical vapor deposition, molecular beam epitaxy, liquid phase epitaxy and close-spaced vapor transport), GaAs or ZnSe single crystal substrates were used. The substrate temperature was 350 to 900°C and the growth conditions were adjusted to obtain an epitaxial deposit. Improvement in the crystalline order in the films may have been a key factor in increasing the film conductivity. In order to understand the role of grain-boundaries and the dependence of film orientation on the conductivity, Ga and Al doped ZnSe films were deposited on oriented single crystal substrates. The substrates were ZnSe (100) and (110), GaAs (100) and ZnS (111). The crystals, $\sim 1\ cm^2$ in area, were polished mechanically by using .05 μm alumina powder to give a smooth surface and washed in methanol prior to film deposition. ZnSe and ZnS crystals were undoped and GaAs was doped with Cr. All substrates had resistivities $> 10^8\ \Omega$-cm. For device fabrication, n-type GaAs, doped with Si ($\rho \sim .02\ \Omega$-cm) was used as a back contact to ZnSe.

The model described by Kirk and Raven[2] was used to establish the conditions for epitaxial growth of ZnSe by vacuum evaporation. The authors calculated the free energy of formation per unit molar volume (ΔE^F) of the deposited film. The ZnSe films deposited on single crystals of Ge were examined and the film growth was found to be epitaxial when ΔE^F was between 1050 and 1200 cal cm^{-3}. When the substrate temperature was low or the growth rate was high (higher source temperature) the films were polycrystalline.

In earlier experiments, ZnSe films were deposited at a substrate temperature of 260°C and the growth rate was ~ 0.2 μm/min. The films were

polycrystalline with $\rho > 10^4$ Ω-cm with the highest intensity peak corresponding to (111) orientation irrespective of substrate. To induce epitaxial growth, the growth rate was lowered by an order of magnitude (~ 0.02 µm/min) by decreasing the source temperature from 1040°C to 900°C and increasing the substrate temperature to 400°C. Some of the samples were sealed in fused silica capsules with 5N9 pure Zn shots and heated at 600°C for 2 hours. The film resistivity was measured in the dark and under AM-1 illumination by the four point probe method. Ohmic contact to the film was made by sputter deposited Al dots.

The growth conditions, film resistivities before and after Zn annealing and the substrate and film orientations are listed in Table I and Table II. As indicated in the tables, the resistivities of as deposited films in the dark on all the substrates were > 10^8 Ω-cm. Under AM-1 illumination, films on GaAs (100) and ZnSe substrates were in the 10^2-10^4 Ω-cm range. The films were polycrystalline as determined from x-ray diffraction scans although in most cases some degree of preferred orientation was present in films deposited at higher growth rates. Doping with Ga or Al had no measureable effect on conductivity but all undoped films had $\rho > 10^8$ Ω-cm both in the dark and the light.

The film resistivities were reduced by a few orders of magnitude when the samples were annealed in Zn vapor. This is expected as Zn vacancies in ZnSe form complexes with donor impurities and act as traps; annealing in Zn vapor increases the electron concentration by removing these sites. The resistivities were 10^{-1} to 10^{-2} Ω-cm on GaAs (100) and ZnSe (100) substrates, 1-10 Ω-cm on ZnSe (110) substrates, and 10^3-10^4 Ω-cm on ZnS (111) and ZnSe polycrystal substrates. Although the films were polycrystalline with (111)

TABLE I

Resistivities of ZnSe films deposited on single crystal substrates

Sample #	T_{ZnSe} (°C)	$T_{substrate}$ (°C)	Dopant	Growth rate (μm/min)	Substrate	Film Orientation	ρ (Ω-cm) dark	ρ (Ω-cm) light
60035-8	990	400	Ga	.018	ZnSe(100)	-	$> 10^8$	$2x10^3$
60031-4	1040	400	Ga	-	ZnSe(110)	(110)	$> 10^8$	13
60033-8	950	825	Ga	-	ZnSe poly-crystalline	polycrystalline (large grain)	$> 10^8$	$4.1x10^4$
60031-7	1040	400	Ga	-	ZnS(111)	(111)	$> 10^8$	$1x10^6$
60036-4	990	400	Ga	.013	GaAs(100)	-	$> 10^8$	450
60038-6	940	320	Ga	.007	GaAs(100)	polycrystalline	$> 10^8$	136
60035-4	990	400	Ga	.018	Sapphire	polycrystalline	$> 10^8$	$> 10^8$
60035-5	990	400	Ga	.018	7059 Glass	polycrystalline	$> 10^8$	$> 10^8$
60046-4	990	400	Al	.009	ZnSe(100)	polycrystalline	$> 10^8$	$2.6x10^3$
60046-7	990	400	Al	.009	GaAs(100)	polycrystalline	$> 10^8$	$9.1x10^3$
60048-4	990	400	-	-	GaAs(100)	polycrystalline	$> 10^8$	$> 10^8$

TABLE II

Resistivities of ZnSe films after annealing in Zn vapor at 600°C for 2 hours

Sample #	T_{ZnSe} (°C)	$T_{substrate}$ (°C)	Dopant	Growth rate (μm/min)	Substrate	Film Orientation	ρ (Ω-cm) dark	ρ (Ω-cm) light
60045-7	900	400	Ga	.006	ZnSe(100)	-	0.86	0.83
60045-8	900	400	Ga	.006	ZnSe(110)	-	9.1	2.1
60045-9	900	400	Ga	.006	ZnSe poly-crystalline	polycrystalline	3.8×10^4	8.1×10^3
60039-8	990	400	Ga	.018	GaAs(100)	polycrystalline	.01	.01
60050-4	990	400	Al	.026	ZnSe(110)	polycrystalline	4.5×10^3	113
60050-7	990	400	Al	.026	GaAs(100)	polycrystalline	3.8	1.7
60050-9	990	400	Al	.026	ZnS(111)	(111) epitaxial	2.2×10^4	82
60049-8	900	400	-	.033	GaAs(100)	polycrystalline	$> 10^8$	$> 10^8$

orientation being dominant irrespective of the substrate orientation, the film resistivities were clearly dependent on the substrate orientation. Ga appeared to be the most effective dopant as Al doped films had resistivities an order of magnitude higher than in Ga doped films. Annealing in Zn vapor had no effect on the films that were not doped during deposition.

4.3 Zn_3P_2/ZnSe Heterojunction Devices

Zn_3P_2/ZnSe devices were prepared on low resistivity ZnSe films. As described in the last section, the resistivity of ZnSe could be lowered to $\lesssim 1$ Ω-cm only if the films were deposited on GaAs or ZnSe oriented single crystals and annealed in Zn vapor at 600°C. For device purposes, Si doped n-type GaAs Single crystals ($\rho \sim 0.02$ Ω-cm) were used as substrates as GaAs also made on ohmic contact to ZnSe.

Thin films of Zn_3P_2 were deposited on ZnSe films by CSVT. The Zn_3P_2 source temperature was 635°C, the substrate temperature was 500°C. The deposition was carried out in argon atmosphere and the growth rate was estimated to be ~ 0.2-0.3 μm/min. Table III lists the process parameters for four Zn_3P_2/ZnSe devices.

The device area (0.1 cm^2) was defined by photolithography and the Zn_3P_2 and ZnSe films were removed from the region not protected by the photoresist (Kodak 747) by etching in Br-MeOH. A small dot of Au was evaporated on the Zn_3P_2 film to make an ohmic contact to it. Contact to the ZnSe side was made by using an In solder on GaAs and heating it to ~ 150°C. The device configuration was as shown in the diagram below:

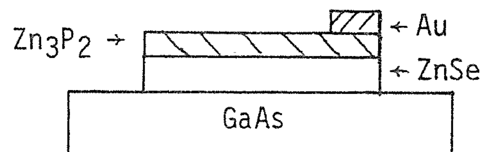

The I-V characteristics were measured in dark and under simulated AM-1 illumination (ELH lamp, 87 mW/cm^2) as shown in Figure 1. A maximum V_{oc} of 0.81 volt and J_{sc} of 1.6 mA/cm^2 was observed. The fill factor was ~ 0.5-0.6 and the series resistance of the device was higher than expected. This may be due to high back contact resistance. The cell parameters are listed in

TABLE III

Preparation Conditions for $ZnSe/Zn_3P_2$ Devices

Sample #	ZnSe Deposition				Zn Anneal	Zn_3P_2 Deposition		
	T_{ZnSe} (°C)	T_{Ga} (°C)	$T_{substrate}$ (°C)	Growth rate µm/min.		$T_{Zn_3P_2}$ (°C)	$T_{substrate}$ (°C)	Growth time (min)
60039-7	990	850	400	.012		635	500	5
60039-9	990	850	400	.012	600°C for	635	500	5
60041-4	980	850	400	.015	2 hours	635	500	3
60041-6	980	850	400	.015		635	500	3

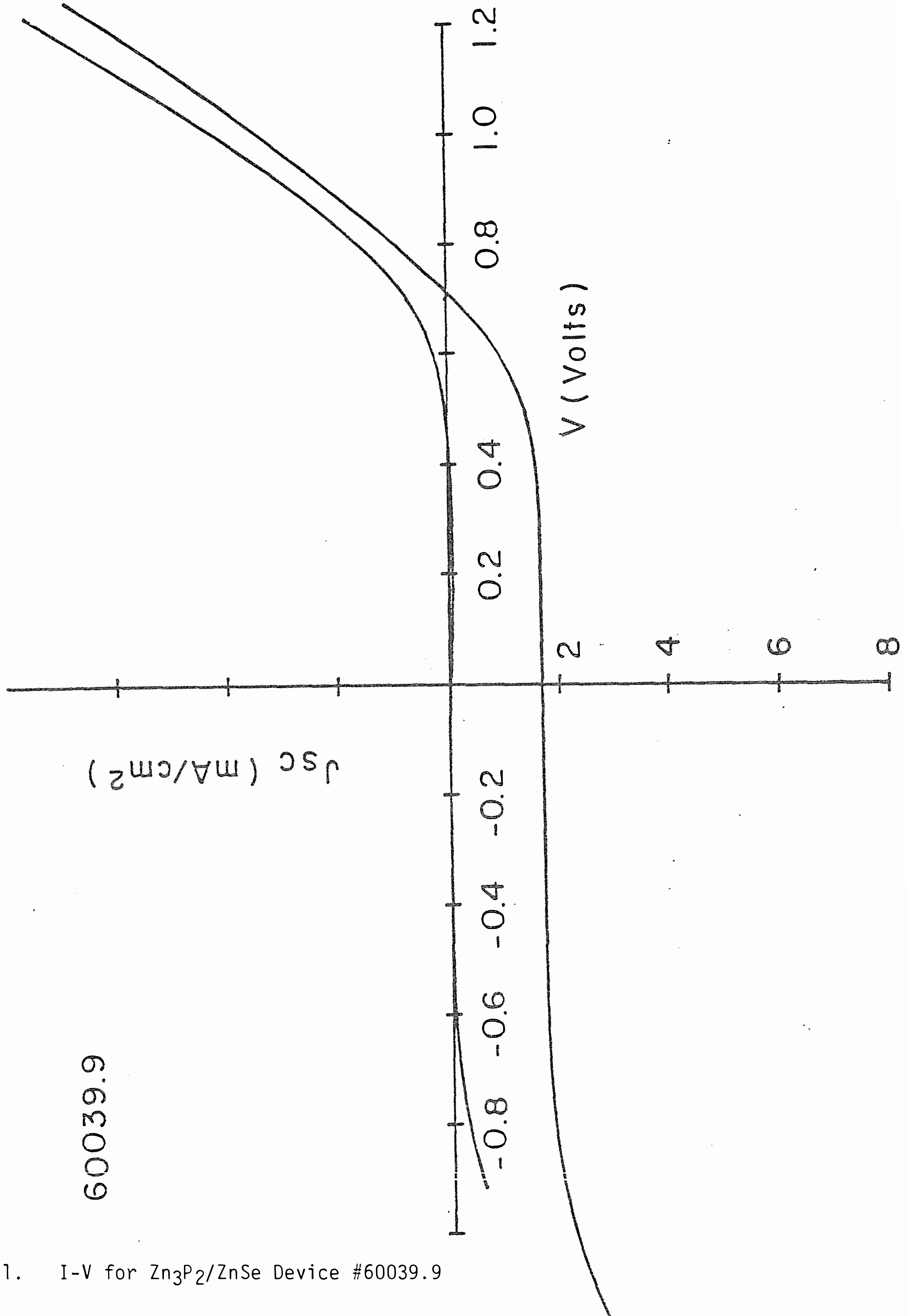

Figure 1. I-V for Zn_3P_2/ZnSe Device #60039.9

Table IV. Laser scans of the device showed that the current was being generated uniformly over the device area. This indicated that the sheet resistance of the Zn_3P_2 film was very low and did not contribute to the series resistance of the device.

The spectral response characteristics of this device are shown in Figure 2. The carriers generated by light of wavelength < 700 nm are not collected efficiently due to high surface recombination velocity and small diffusion length in Zn_3P_2. The Zn_3P_2 film thickness is estimated to be ~ 1-2 µm which is comparable to the electron diffusion length in Zn_3P_2 films deposited on mica or silicon steel substrates. However, it has been found earlier that Zn_3P_2 films deposited on GaAs substrates have shorter electron diffusion lengths (~ 0.1 µm) probably due to interdiffusion of the two materials at the high substrate temperature during film deposition. An improvement in the light generated current is expected if the Zn_3P_2 film is < 1 µm thick.

The diffusion voltage V_D of the Zn_3P_2/ZnSe heterojunction was determined from the temperature dependence of V_{OC} (Figure 3). The slope of V_{OC} vs temperature plot was 2.43 mV/°C and V_D was estimated to be 1.48 volts. The short-circuit current, J_{SC}, and V_{OC} were measured as a function of light intensity with the aid of neutral density filters. As shown in Figure 4, the J_{SC} vs V_{OC} plot showed a double diode. The diode factor was 2.4 and the reverse saturation current was 5.4×10^{-8} Amp/cm^2 for V > 0.4 volt.

Capacitance-voltage measurements were made in the frequency range of 0.1 to 4 KHz. The barrier height was estimated from the intercept of $1/C^2$ vs voltage plot. The barrier height was found to be ~ 1.3 eV in the dark and

TABLE IV

Zn_3P_2/ZnSe Device Parameters

Sample #	J_{sc} (mA/cm²)	V_{oc} (Volts)	FF	η (%)	R_S (Ω-cm²)	R_{SH} (Ω-cm²)
60039-7	0.45	0.65	0.50	0.2	130	6×10^4
60039-9	1.67	0.71	0.57	0.77	80	$> 10^5$
60041-4	0.94	0.81	0.62	0.54	150	$> 10^5$
60041-6	1.55	0.81	0.50	0.8	180	$> 10^5$

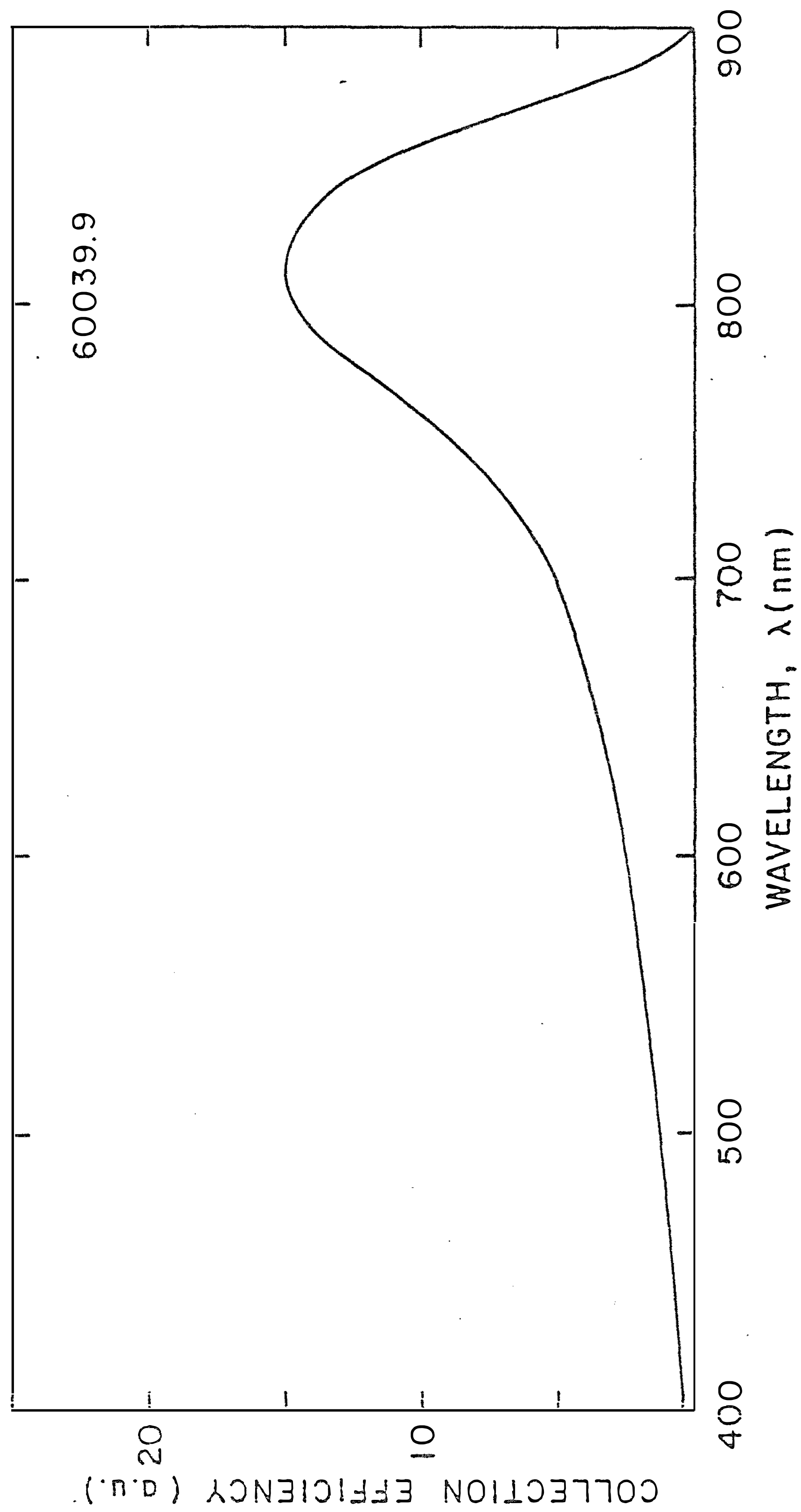

Figure 2. Spectral Response for Zn_3P_2/ZnSe Device #60039.9

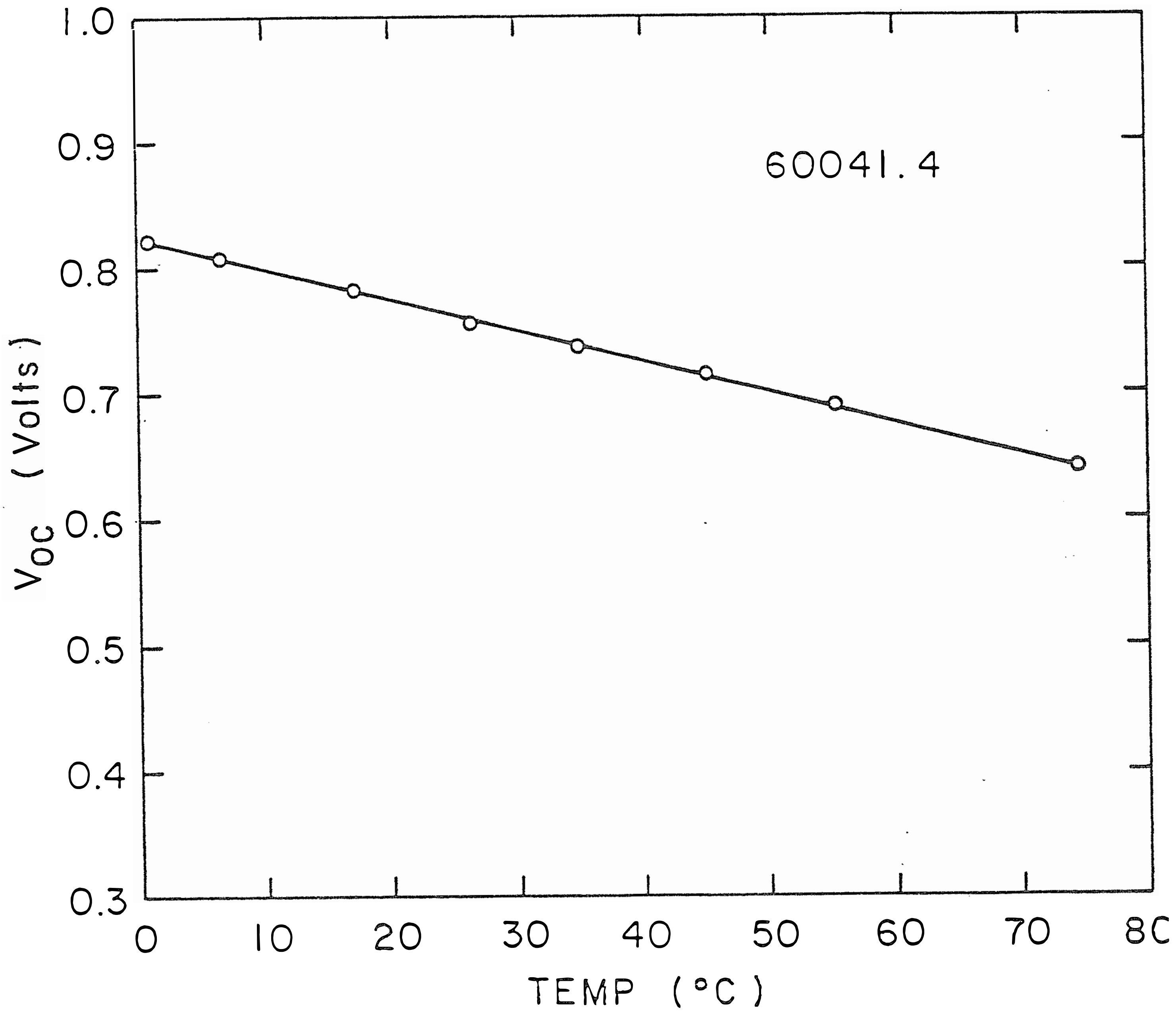

Figure 3. Temperature Dependence of the Open Circuit Voltage for Zn_3P_2/ZnSe Device #60041.4

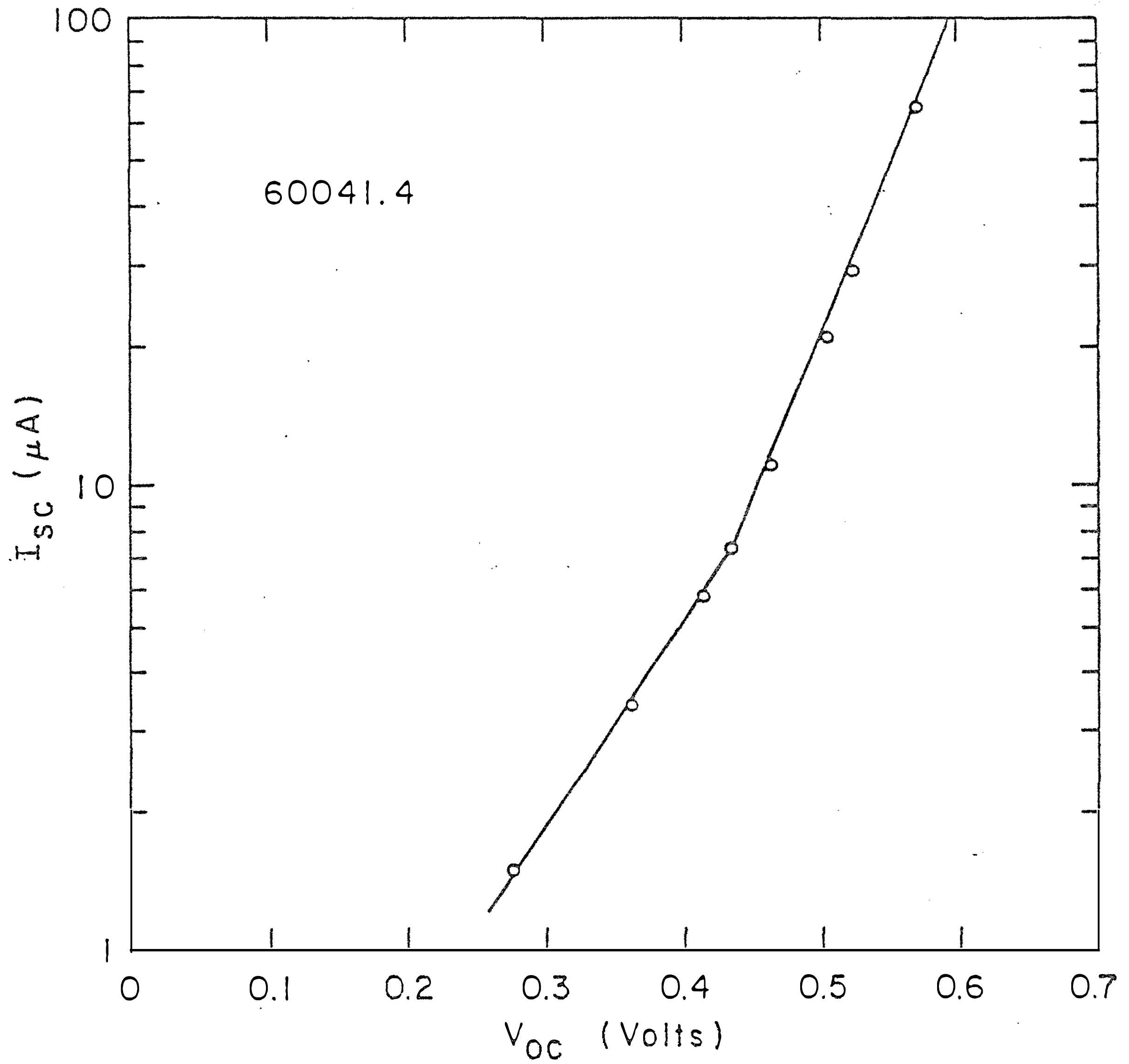

Figure 4. I_{sc} vs V_{oc} for Zn_3P_2/ZnSe Device #60041.4

~ 1.2 eV under AM-1 illumination. The depletion layer width in the device, calculated from the capacitance at zero voltage bias was 0.04 μm. This is in accordance with the spectral response plot as due to a small space charge region in the device, the carriers are collected by diffusion and those generated near the surface are unable to reach the junction.

5. Zn_3P_2/(CdZn)S Heterojunction Devices

The increased bandgap and change in electron affinity that occurs as Zn is substituted for Cd in CdS has been utililzed with benefit in a number of photovoltaic systems. The increased bandgap results in a potentially higher light generated current and changing the electron affinity to more closely match the absorber has been shown in the Cu_2S/CdS system to result in an increased open circuit voltage. With both $CuInSe_2$ and Cu_2S, the zinc concentrations successfully used have been relatively low whereas optimum for Zn_3P_2 would appear to be in excess of 60% ZnS.[3] At these zinc contents, the resistivity of the (CdZn)S is extremely high and in fact has proved to be a major obstacle to producing high efficiency Zn_3P_2/(CdZn)S devices.

(CdZn)S film growth and post deposition annealing treatments are described and correlated with resulting film properties. Various approaches tried in an effort to overcome the excessive resistivity of high zinc content films are discussed. It was found possible to substantially improve the open circuit voltage of the CdS/Zn_3P_2 heterojunction but it has proved impossible within the contract period to achieve both high voltages and high current.

5.1 $Cd_{1-x}Zn_xS$ Thin-Film Deposition

Thin films of $Cd_{1-x}Zn_xS$ were deposited by thermal evaporation of CdS and ZnS powders from two concentric sources in a vacuum system capable of operating at a pressure of 10^{-6} Torr. The source bottle (Figure 5) was made of graphite and was placed in a two zone heater. The CdS powder was loaded in the lower chamber. The temperatures of the two sources were recorded and controlled independently by thermocouples as shown. The films were doped with indium by co-evaporation from a separate source. Nine 1" x 1" substrates could be placed in the substrate holder which was heated radiatively. The substrate temperature was controlled from a thermocouple embedded in a 7059 glass slide and placed in the substrate holder. The source-to-substrate distance was varied between 12 and 20 cm to achieve the desired growth rate.

The vapor pressures, p (in atmospheres) of CdS and ZnS at a temperature T are given by

$$P_{CdS} = 2.87 \times 10^7 \exp\left[-\frac{2.31}{kT}\right] \quad (1)$$

and

$$P_{ZnS} = 4.21 \times 10^7 \exp\left[-\frac{2.74}{kT}\right] \quad (2)$$

The number of molecules evaporating per unit area per unit time is

$$G = \alpha P \left[\frac{M}{2\pi RT}\right]^{\frac{1}{2}} \quad (3)$$

where α is the evaporation coefficient, and M is the molecular weight of the evaporating species and R is the universal gas constant.

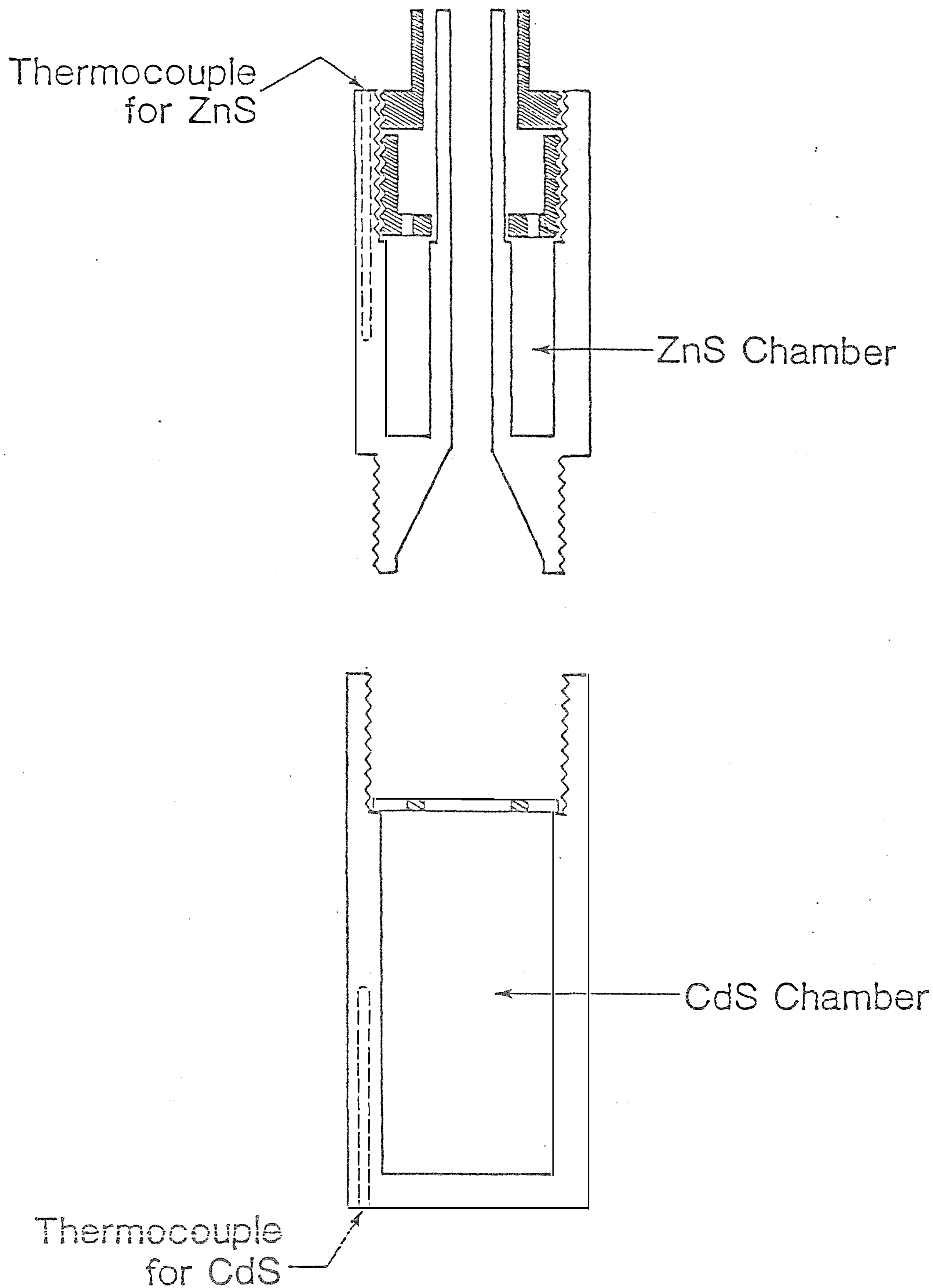

Figure 5. Graphite source bottle for $Cd_{1-x}Zn_xS$ thin-film deposition.

The film thickness, t, is dependent on the molecular flux arriving at the substrate, the sticking coefficient, S a function of the substrate temperature, and the source-to-substrate distance, d, such that:

$$t = \frac{GS\psi}{4\pi d^2 \rho} \tag{4}$$

where the factor ψ takes into account the geometry of the system and ρ is the density.

All depositions were carried out at a substrate temperature of 200°C. Assuming that the evaporation and sticking coefficients for CdS and ZnS are equal, the film composition should be the same as that of the vapor species and is given by the expression:

$$x = \frac{G_{ZnS}}{G_{CdS} + G_{ZnS}} \tag{5}$$

Ideally, the composition is then only dependent on the two source temperatures which in the system used here are to some extent coupled. The CdS and the ZnS sections of the source bottle were weighed before and after the evaporation to determine the effused masses. A calibration curve was then generated from these effused masses and the composition of the deposited film on 7059 glass (Figure 6). It is seen that within the scatter of the data, the film composition is equal to the molecular composition of the flux.

The film thicknesses were measured on a Dektak profilometer. The growth rates were in the range of 0.2 μm to 0.5 μm/min. The average grain size in 10 μm thick CdS films was of the order of a few microns decreasing with increasing zinc concentration so that pure ZnS films had submicron grains.

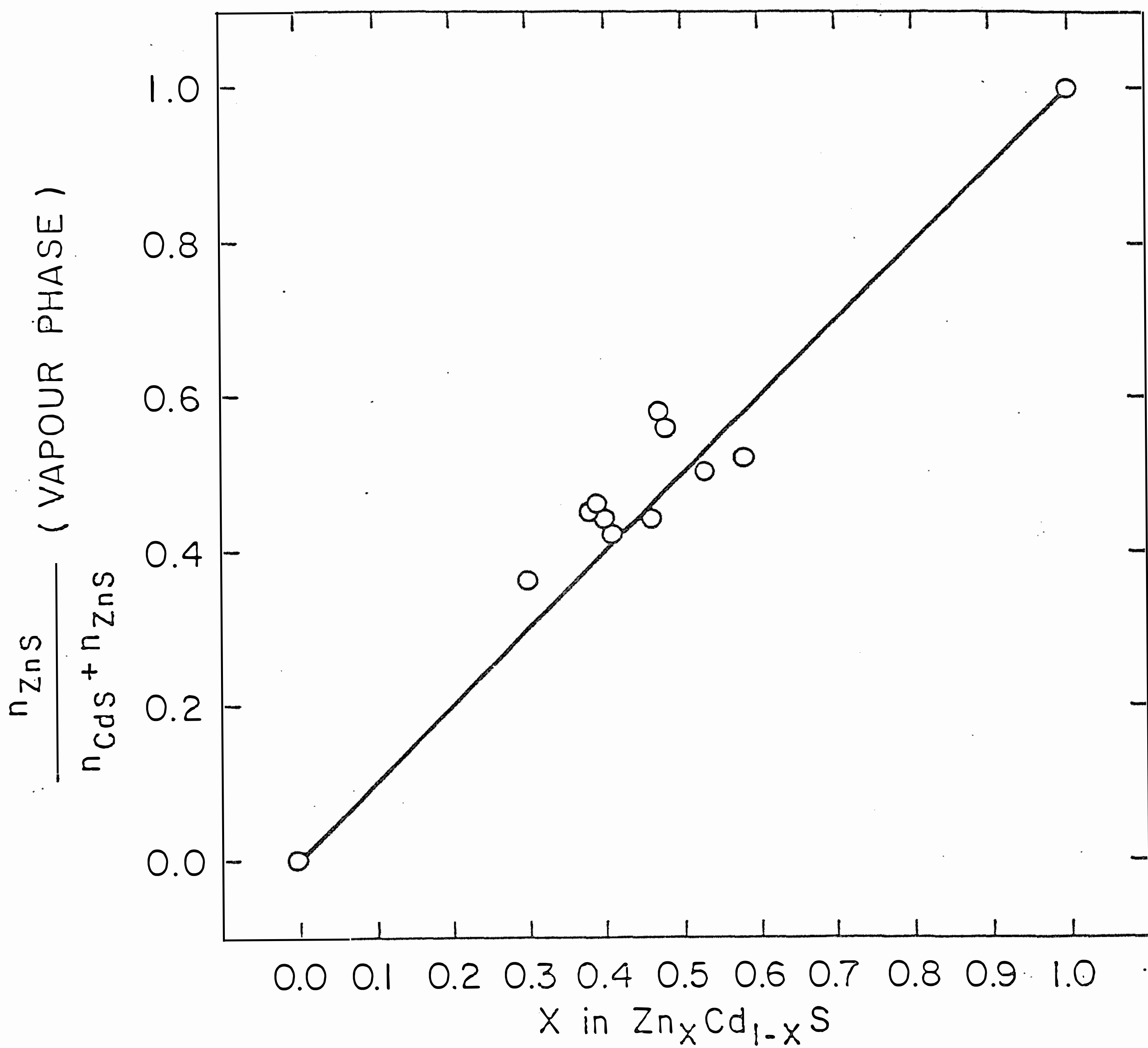

Figure 6. Molecular Composition of the Flux vs $Cd_{1-x}Zn_xS$ Film Composition

X-ray diffraction scans of the films deposited on 7059 glass showed the c-axis to be perpendicular to the plane of the substrate. The lattice constant 'c' was calculated from the (0002) and higher order diffraction peaks. The crystal structure of vapor deposited CdS is hexagonal (wurtzite) whereas pure ZnS films are cubic (zinc blende). The transition from hexagonal to cubic structure takes place in the range of 65-85% Zn[4]. As the lattice constant changes linearly with composition, the Zn concentration in the film for $0 < x < 0.8$ can be determined from the relation

$$x = 2.1667\ c + 14.548 \qquad (6)$$

where c is the lattice parameter[5]. The precision in the measurement of d-spacings increases with the Bragg angle of reflection and it is necessary to consider diffraction peaks at angles > 80° to obtan an accuracy of < ± 1%.

For $x > 0.4$, diffraction peaks corresponding to (105), (106) and (107) were also present showing a significant distribution of basal planes away from the substrate plane.

The dark resistivities of $Cd_{1-x}Zn_xS$ films deposited on glass slides were measured by four point probe. The resistivity increased with x as shown in Figure 7. The resistivity of the CdS films was strongly dependent on the level of indium doping with the resistivity of undoped films five orders of magnitude higher than of those co-evaporated with In at a temperature of 900°C. At higher Zn concentrations ($x > 0.3$), raising the In source temperature from 900°C to 1000°C had no effect on the resistivity. For films with $x > 0.7$, the resistivity was too high to be measurable.

The films deposited on glass slides were heated in argon, hydrogen and vacuum at temperatures ranging from 200°C to 300°C for several hours. The

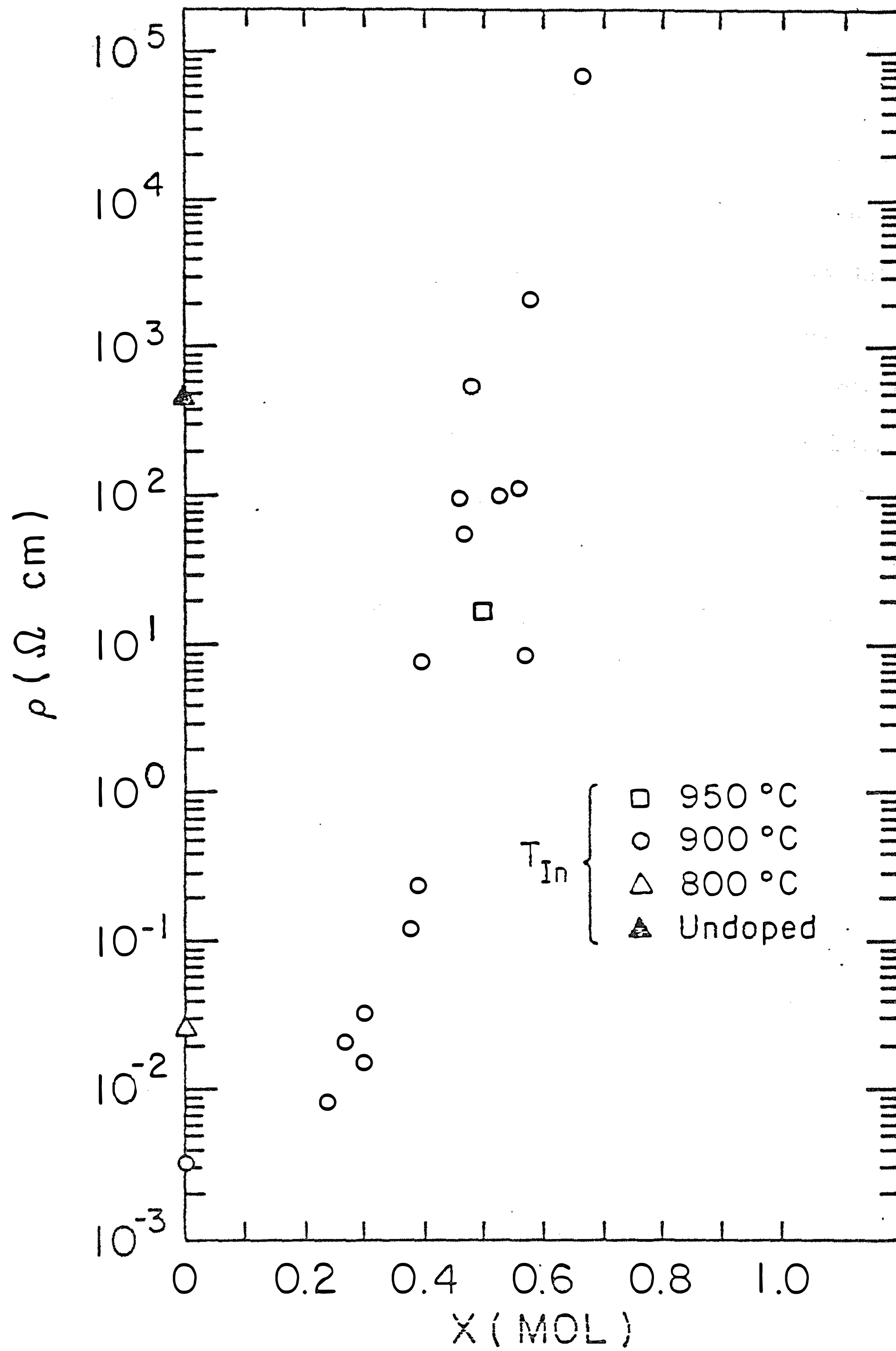

Figure 7. $Cd_{1-x}Zn_xS$ Film Resistivity vs Film Composition

resistivities of the films were measured before and after heating. As shown in Figures 8-10, the resistivities of films with greater than 30% Zn apparently increased by several orders of magnitude as a result of heating. Optical absorption measurements showed that the compositions of the films remain unchanged. Further investigation would be necessary to exclude surface and contact effects as the cause of the observed changes.

(CdZn)S films were also deposited at a substrate temperature of 125°C. The films were highly oriented and had resistivities comparable to those deposited at a substrate temperature of 200°C. The optical transmission was high (65% for a 6 μm thick film) and no evidence of Cd precipitation in the films was observed. It was not possible to lower the substrate temperature further as radiation from the source maintains the substrate at $\geq$ 125°C.

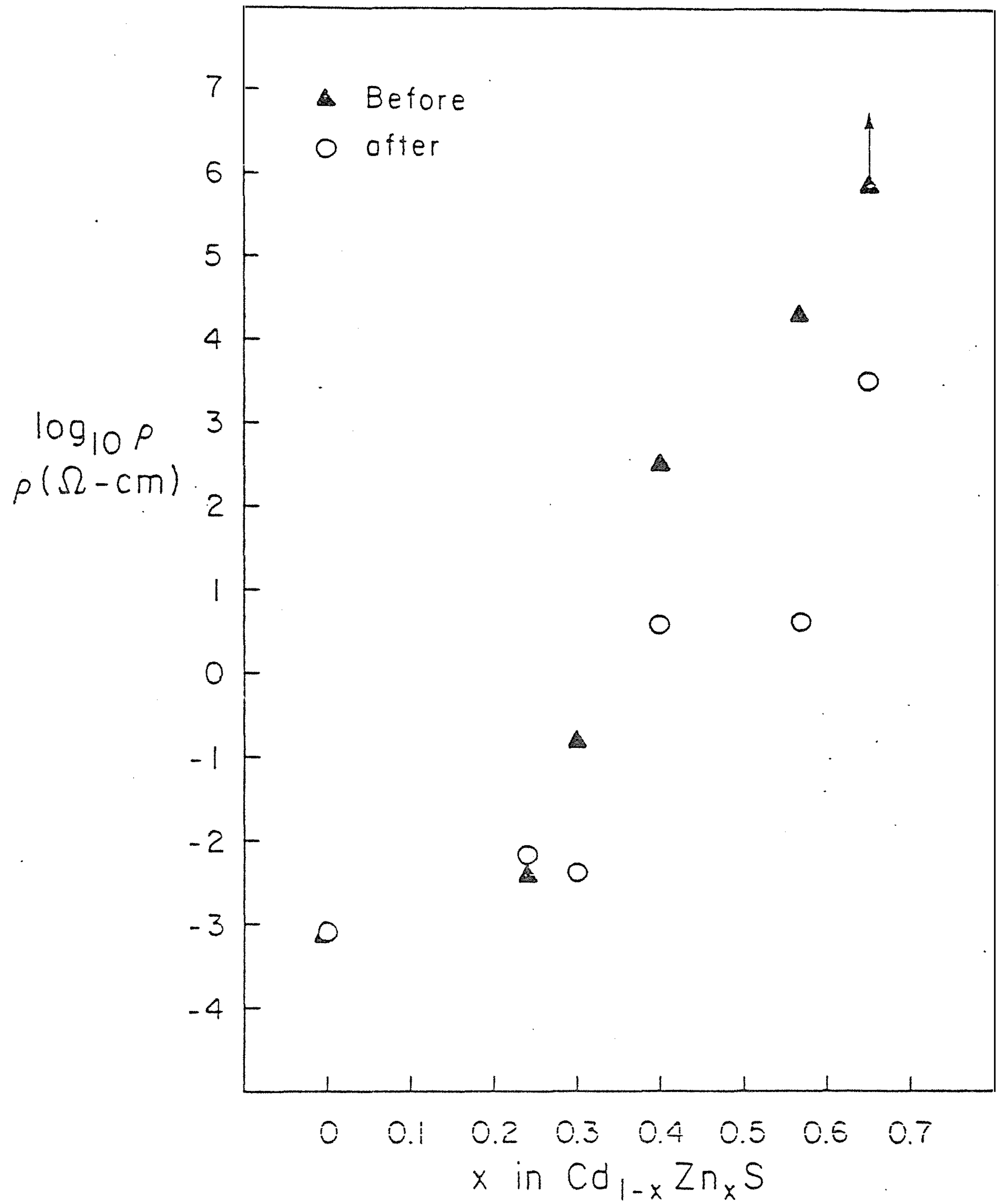

Figure 8. Influence of Heat Treatment in Hydrogen at 200°C for 16 Hours on the Resistivity of (CdZn)S Films

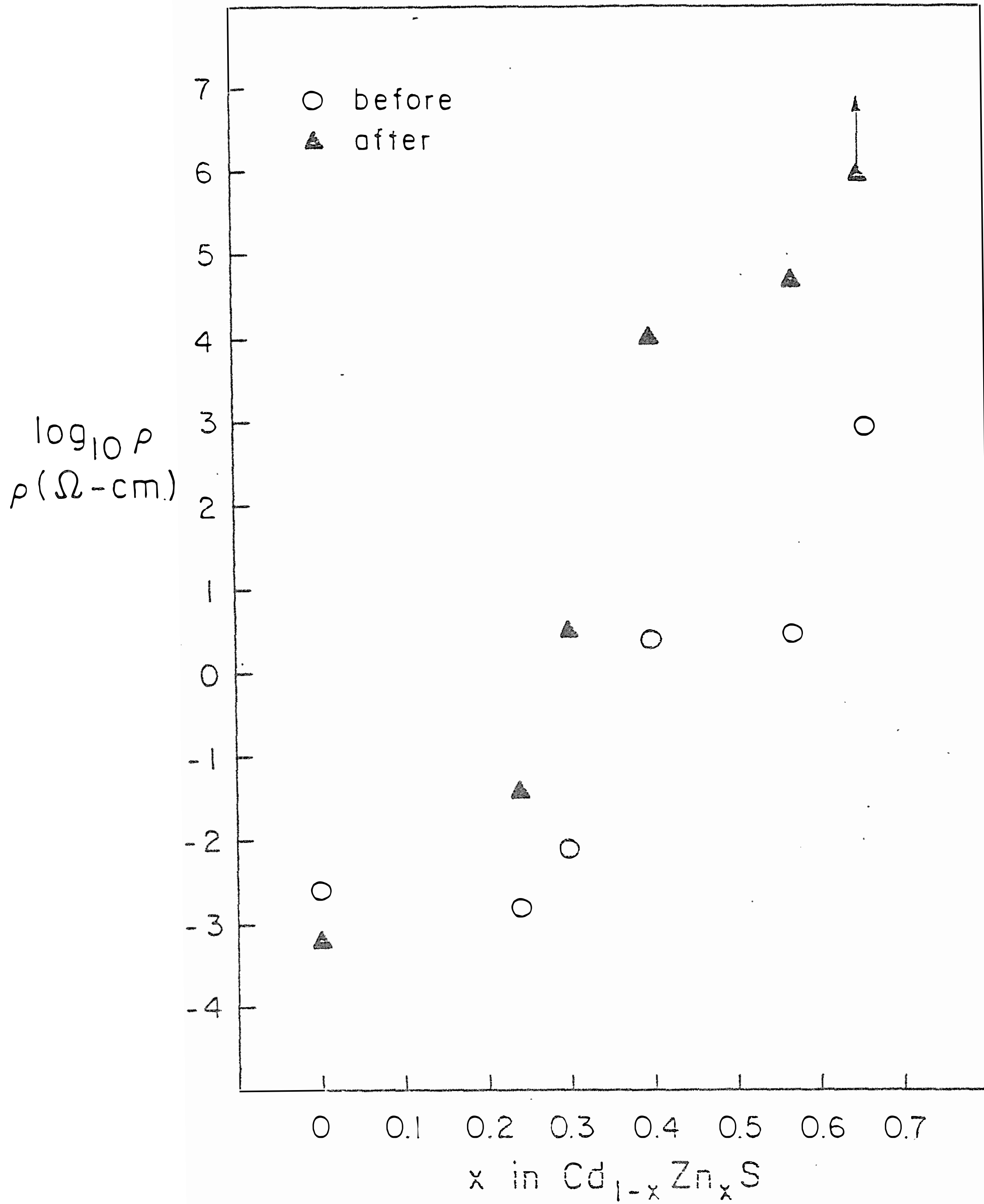

Figure 9. Influence of Hydrogen Heat Treatment at 250°C for 16 hours on the Resistivity of (CdZn)S Films

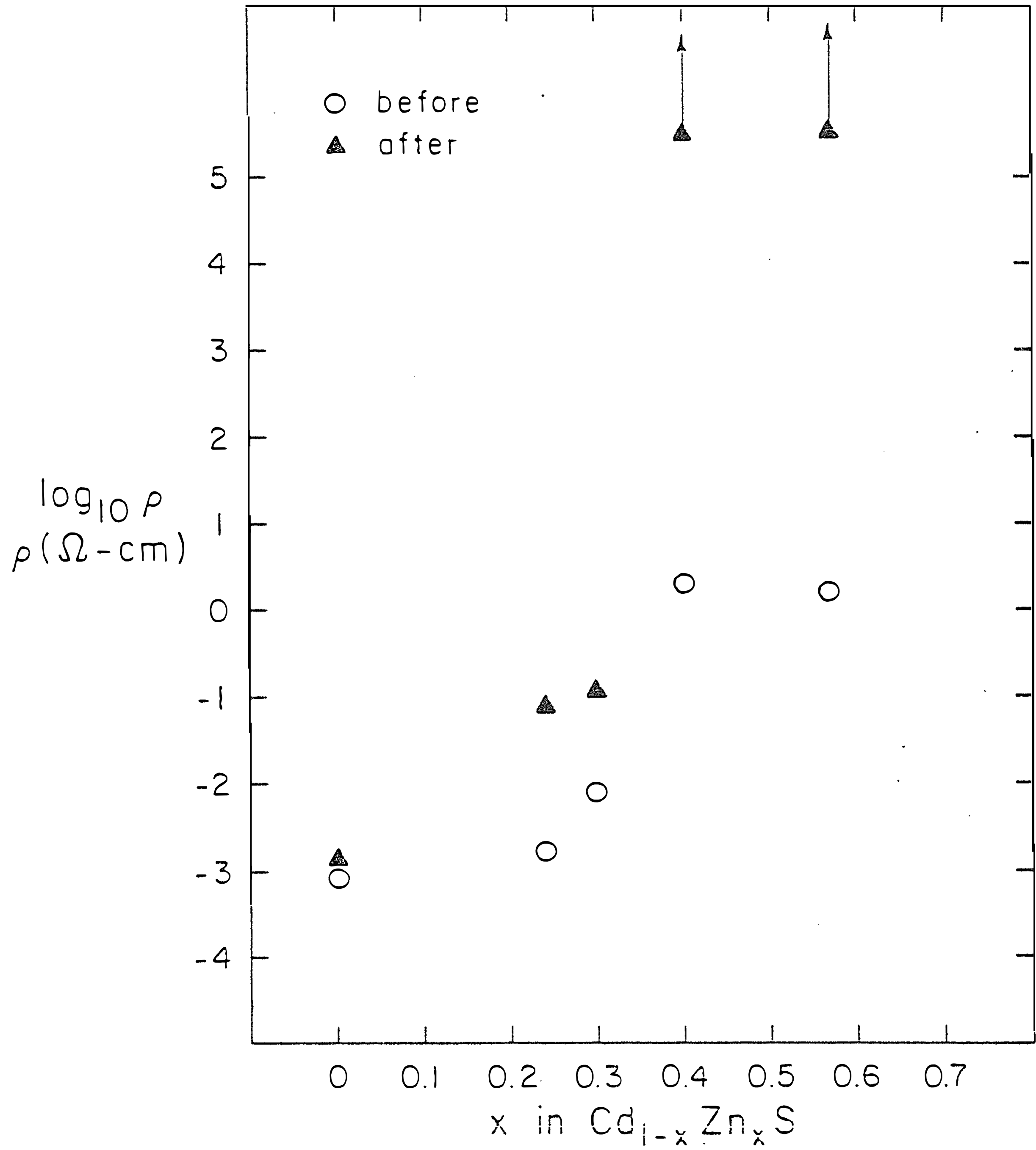

Figure 10. Influence of Vacuum Heat Treatment at 250°C for 16 hours on the Resistivity of (CdZn)S Films

5.2 $Cd_{1-x}Zn_xS/Zn_3P_2$ Devices

Large grain polycrystalline boules of zinc phosphide were grown by vapor transport as outlined in Reference(6). The boules, 1 cm in diameter, were sliced into 0.75 mm thick wafers and polished mechanically and chemically to remove the saw damage. Thin films of Zn_3P_2 were grown by close spaced vapor transport (CSVT) on Fe/Si coated mica substrates(7). The samples were etched in a solution of Br in methanol to remove any oxide layer on the surface and to obtain a smooth surface just prior to depositing the $Cd_{1-x}Zn_xS$ film.

Thin films of indium doped $Cd_{1-x}Zn_xS$ were deposited on Zn_3P_2 wafers at a substrate temperature of 200°C monitored by a thermocouple bonded to a Zn_3P_2 wafer. The indium source temperature was kept at 900°C and the temperatures of the CdS and the ZnS sources were set to give the desired film composition. Ohmic contact to (CdZn)S was made by a 100 nm thick film of sputter deposited indium tin oxide (ITO). The device area (0.1 cm^2) was defined by photolithography and the ITO and (CdZn)S in the unprotected regions were removed by dissolving in dilute HCl. A 200 nm thick film of Ag was evaporated on the back surface of the Zn_3P_2 to make ohmic contact to it. For devices on thin-films of Zn_3P_2 an Fe/Si layer on the substrate served as ohmic contact.

In each run, a clean glass slide was also placed in the substrate holder. This sample was used to monitor the composition, thickness and resistivity of the $Cd_{1-x}Zn_xS$ films. X-ray diffraction scans of the films deposited on Zn_3P_2 substrates showed that the film compositions were the same as those on the glass slides within the error of measurements. The film thicknesses however were different, possibly due to small differences in the substrate temperatures influencing the sticking coefficients.

Current-voltage characteristics were measured in the dark and under simulated AM-1 illumination (ELH lamp, 87.5 mW/cm^2). Figure 11 shows a typical I-V plot of a (CdZn)S/Zn_3P_2 device (Sample #1791-1). The (CdZn)S film contained 35% Zn and was deposited on a polycrystalline Zn_3P_2 wafer. Figures 12 and 13 show the open-circuit voltage, V_{OC}, in bulk and thin-film samples as a function of $Cd_{1-x}Zn_xS$ film composition. It would appear that by improving the electron affinity match between the two semiconductors V_{OC} increases. The short circuit current, J_{SC} varied randomly between 0.5 and 6 mA/cm^2. J_{SC} is dependent on the electron diffusion length, the space charge width, i.e. the carrier concentration in Zn_3P_2, the device series resistance and the surface and the interface recombination velocities which vary from sample to sample. All devices showed a light induced low shunt resistance which reduced the fill factor. Full device analysis was performed on bulk samples only.

The diode factor, A, and the reverse saturation current, J_o, were computed from the log I vs voltage plots in the light and dark. Corrections were made for the series and the shunt resistances. The diode factors were unusually high (2 to 3) and J_o decreased from 10^{-4} to 10^{-8} mA/cm^2 as x in the $Cd_{1-x}Zn_xS$ films increased from 0 to 0.66, Figure 14.

The I-V characteristics of sample #1791-1 were measured at temperatures ranging from -140°C to +80°C. V_{OC} varied linearly with temperature in the range of -100°C to +80°C, Figure 15, and a diffusion voltage of 0.71 volt was extracted from this data. J_o in the dark and light decreased as the temperature was lowered, Figure 16.

The collection efficiency was reduced under AM-1 bias light, Figure 17. However, the ratio of collection efficiencies measured with and without light bias were independent of the wavelength of the light. This

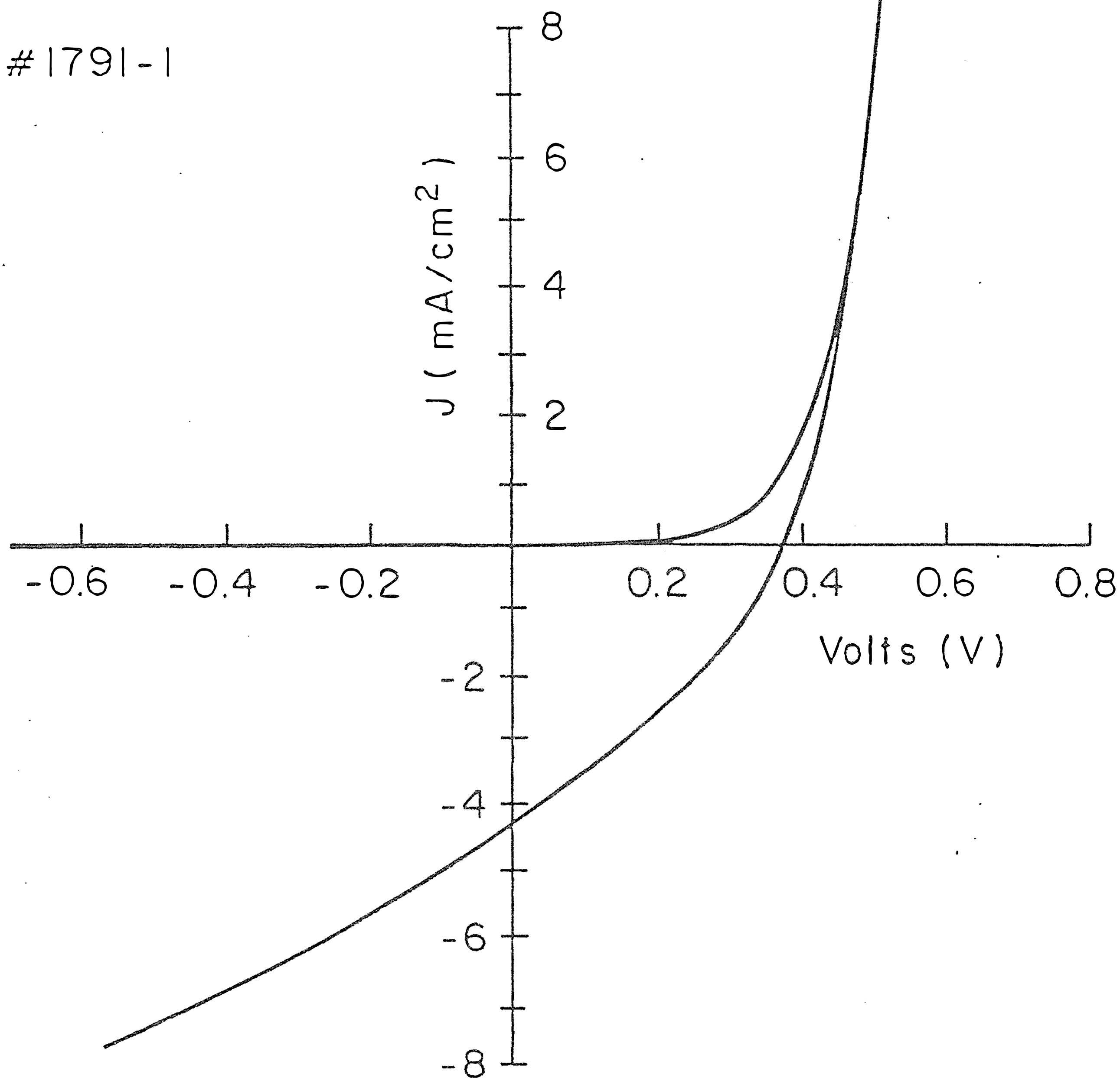

Figure 11. I-V Curve for $(CdZn)S/Zn_3P_2$ Device #1791.1

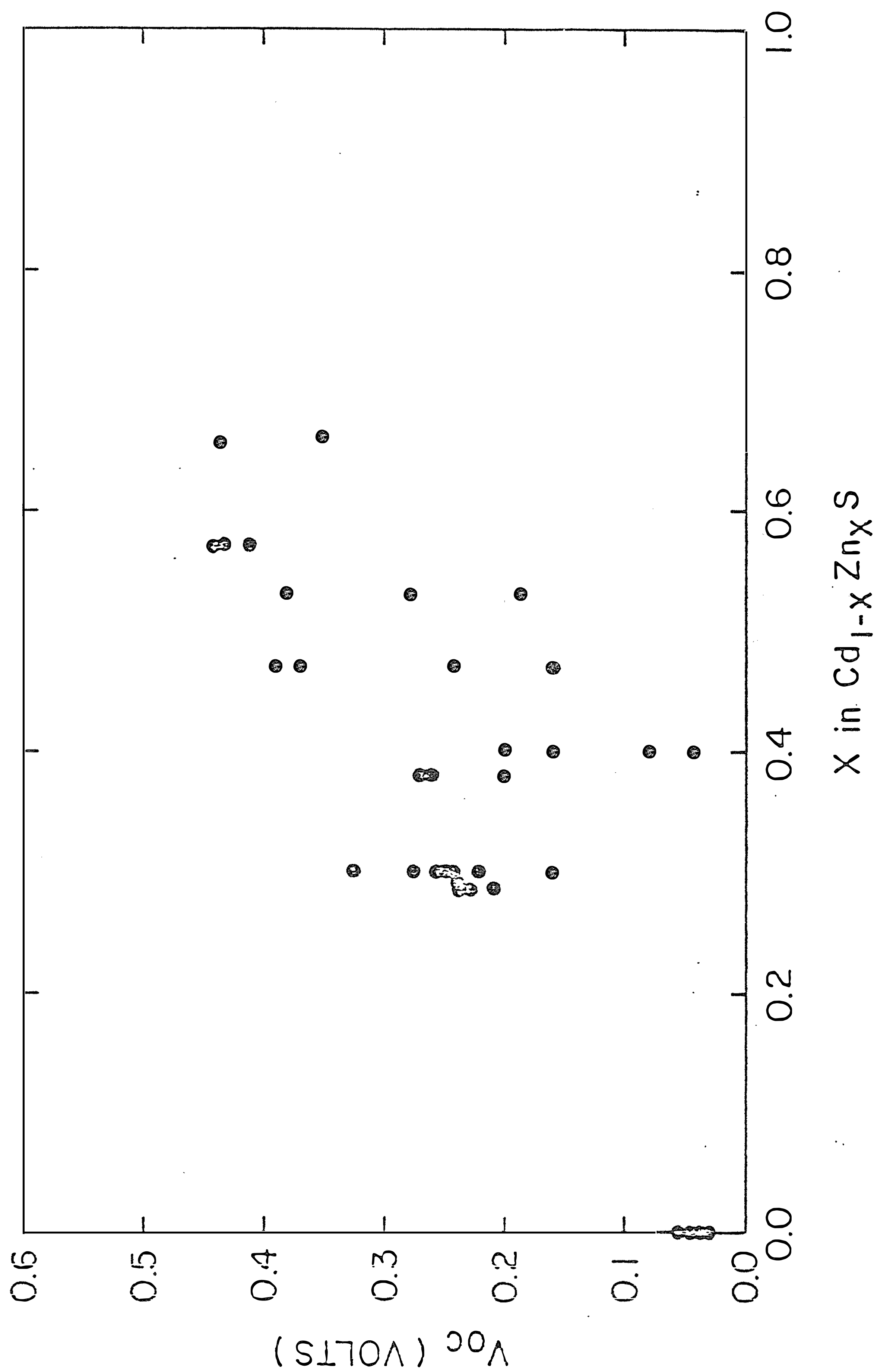

Figure 12. Open Circuit Voltage vs Zinc Content of $(CdZn)S/Zn_3P_2$ Bulk Devices

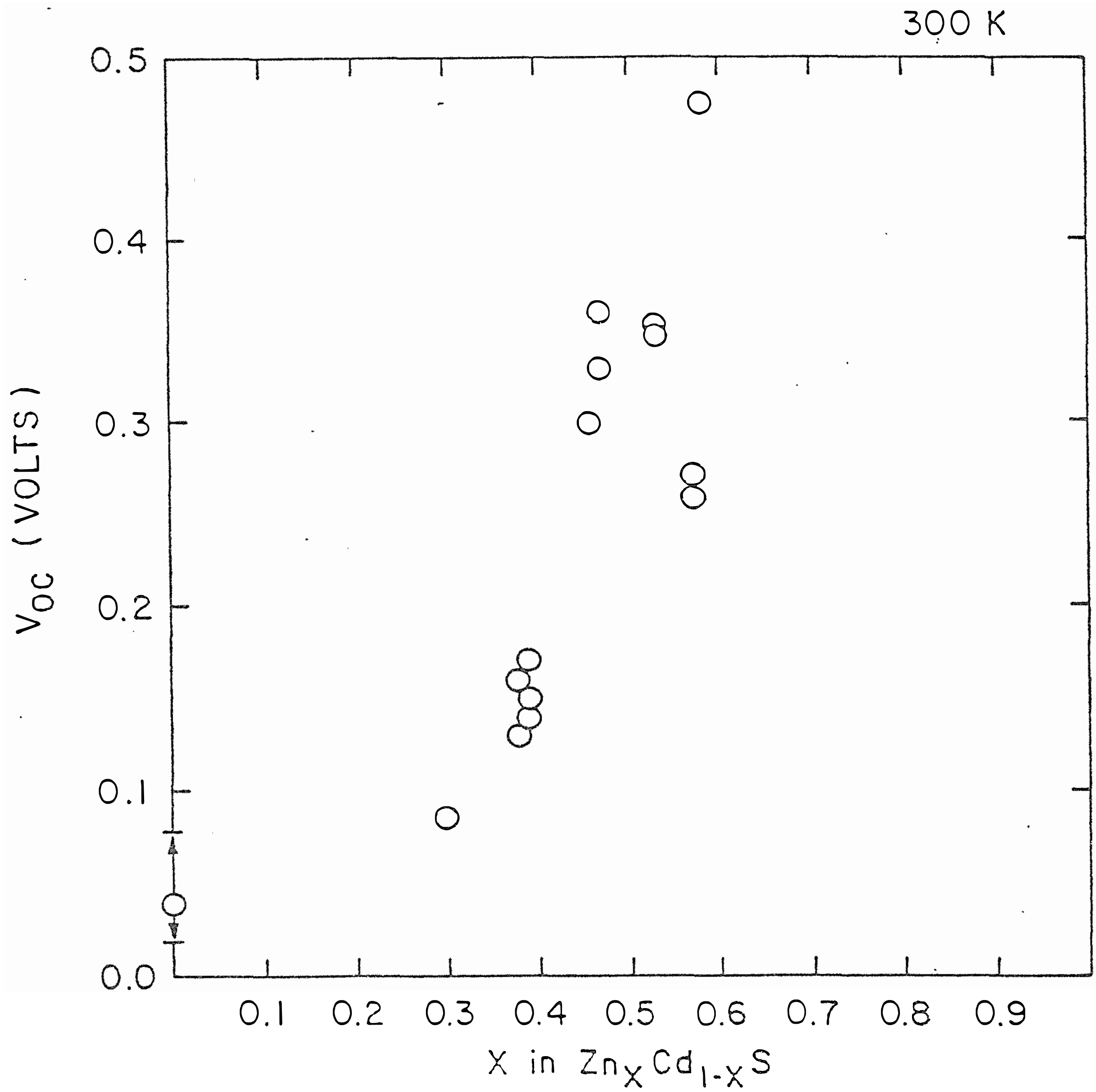

Figure 13. Open Circuit Voltage vs Zinc Content of $(CdZn)S/Zn_3P_2$ of Thin-Film Devices

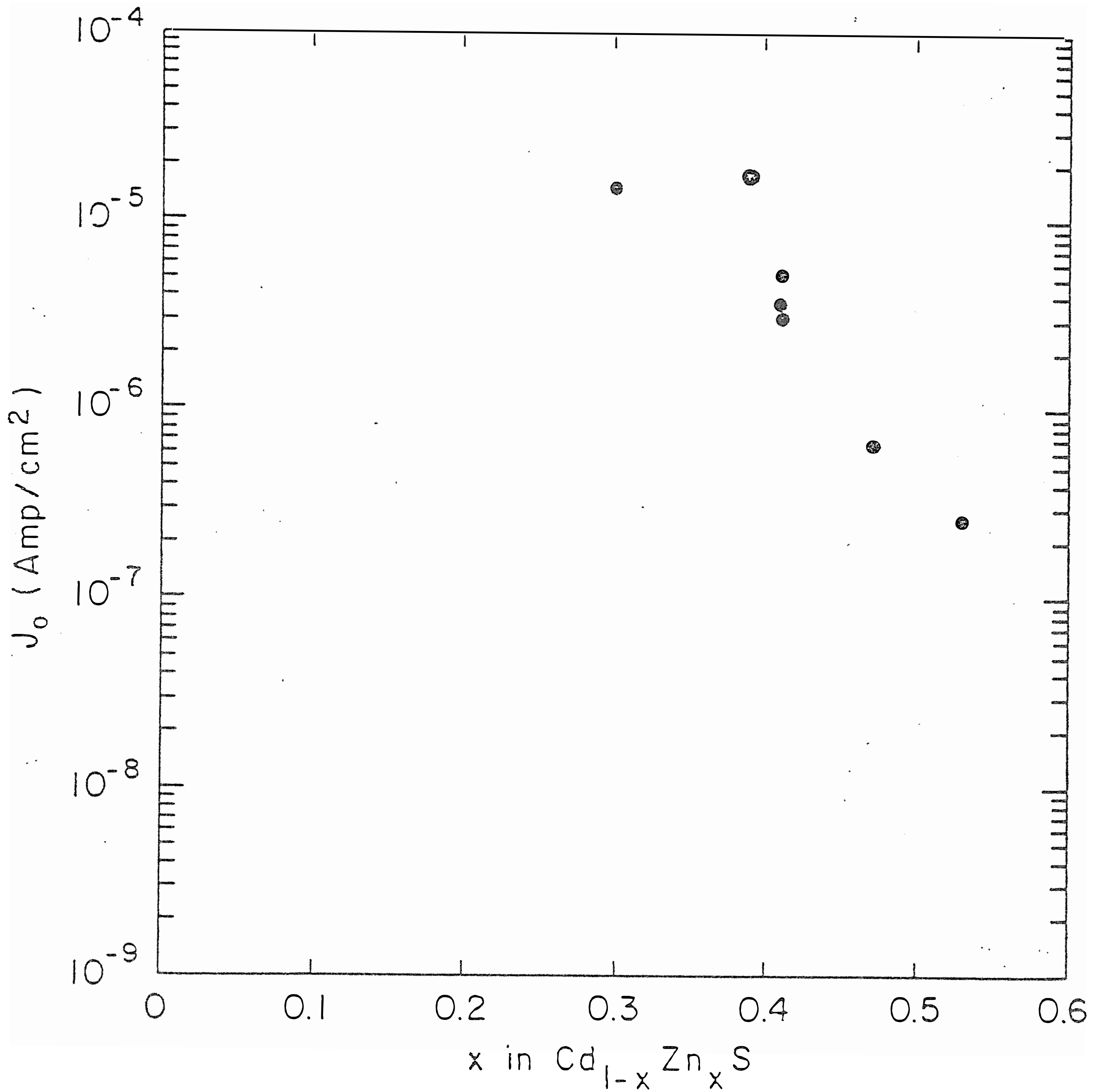

Figure 14. J_o vs Zinc Content of $(CdZn)S/Zn_3P_2$ Devices

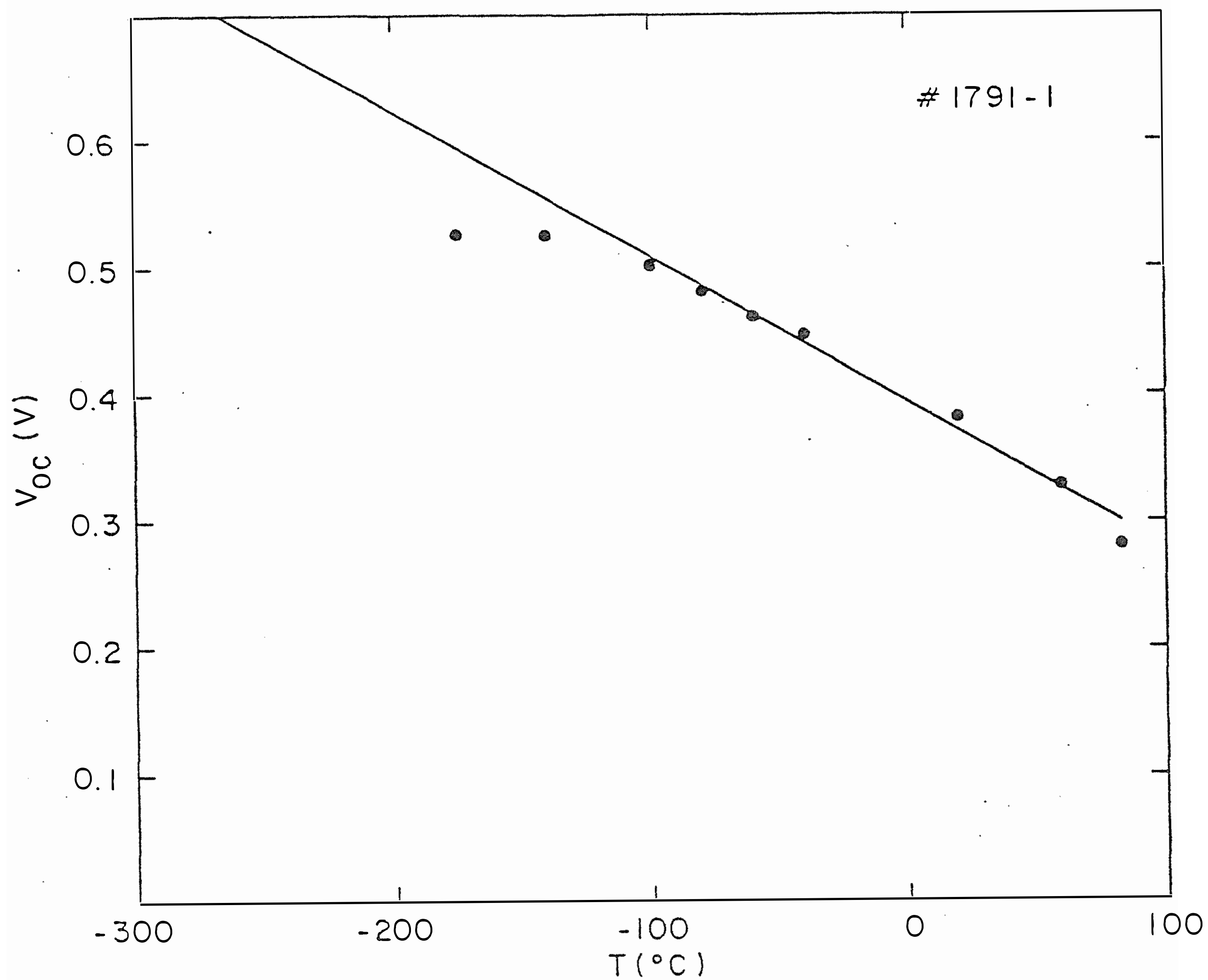

Figure 15. Open Circuit Voltage vs Temperature for $(CdZn)S/Zn_3P_2$ Device #1791.1

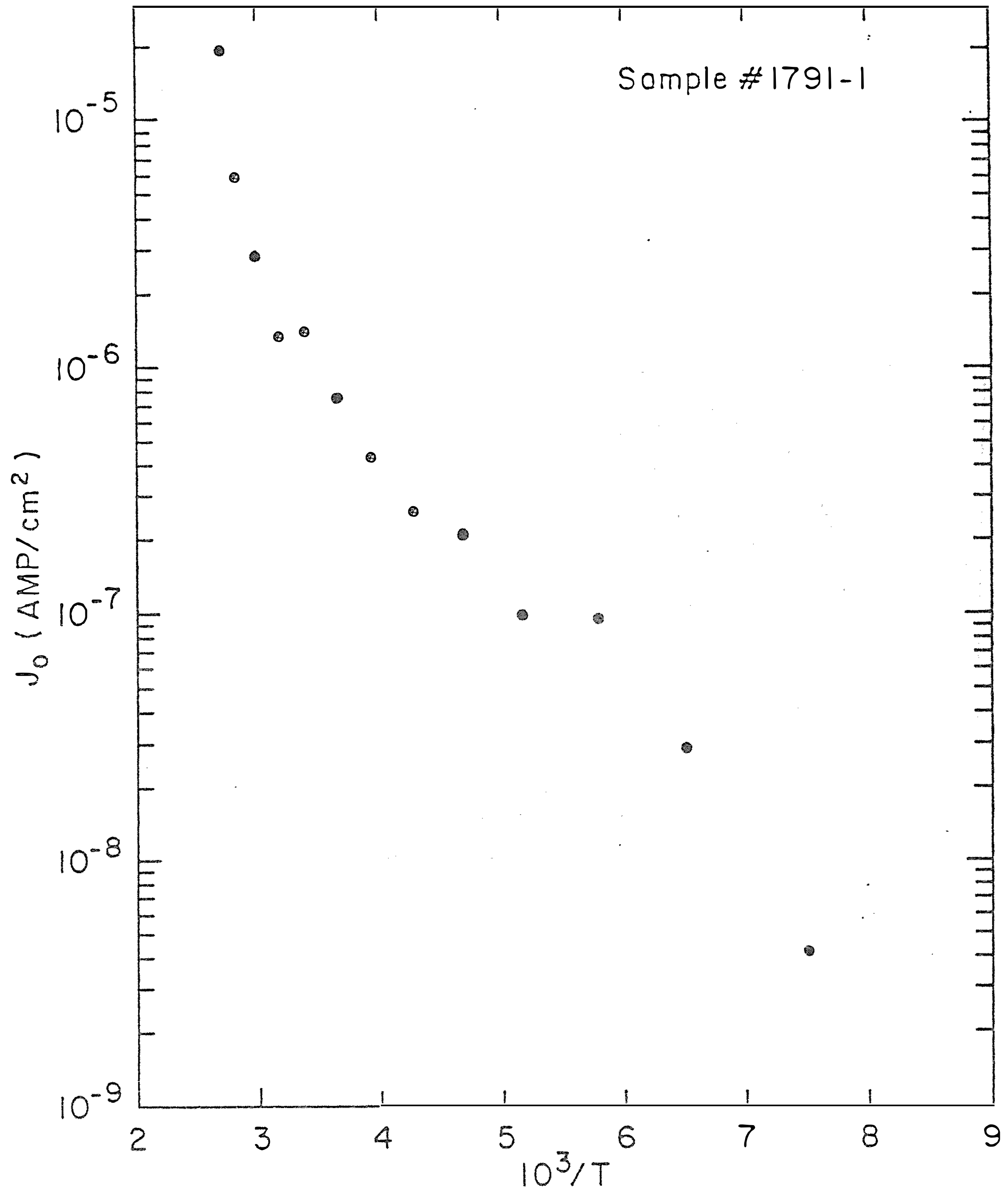

Figure 16. J_0 vs Reciprocal Temperature for $(CdZn)S/Zn_3P_2$ Device #1791-1

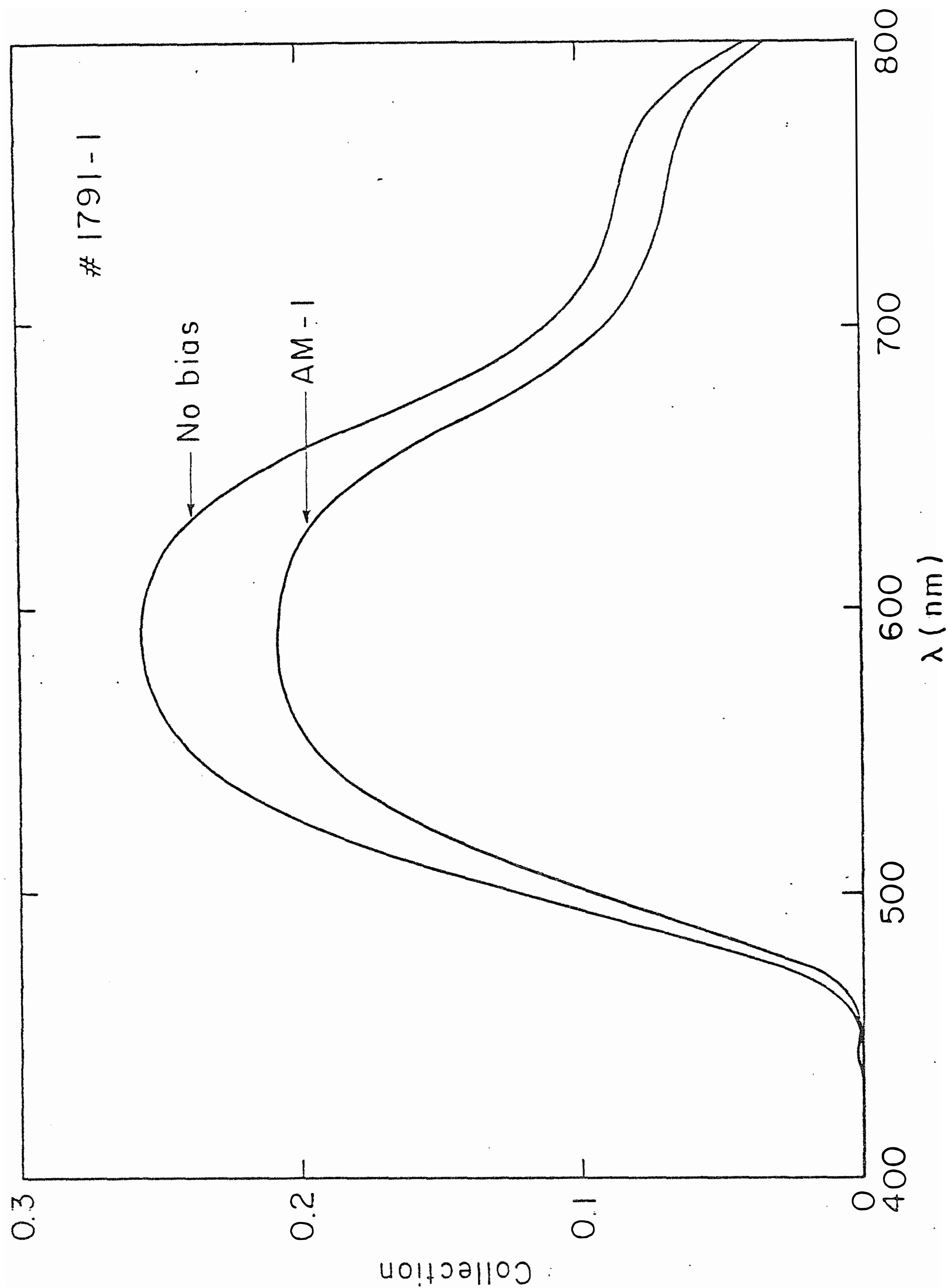

Figure 17. Collection Efficiency as a Function of Wavelength With and Without Bias Light for (CdZn)S/Zn_3P_2 Device #1791-1

indicates that the reduction in collection efficiency with light bias is not due to a decrease in the space charge width. If that were true, the collection efficiencies for short wavelength light will not be affected as this light is always absorbed within the space charge region. This decrease is attributed to the change in the density of the recombination centers in the presence of light.

Figure 18 shows the spectral response measurements on a number of cells with different compositions of the window material. A finite value of the collection efficiency is only obtained for photons of energy smaller than the bandgap of the window semiconductor as expected. The results indicate that the $Cd_{1-x}Zn_xS$ films are not graded in composition and the bandgap varies with x as shown by the optical absorption measurements. The collection efficiency is fairly uniform for the carriers generated in Zn_3P_2 except near its absorption edge where the absorption length becomes comparable to the minority carrier diffusion length.

As the short circuit current in all the devices was lower than the theoretically predicted value, laser spot scans were made to check the spatial uniformity of the devices. A focused He-Neon laser beam of wavelength 6328 Å was used as it is not absorbed by the (CdZn)S front layer. As shown in Figure 19 the cell has a fairly uniform response over the device area with a low density of defects.

A cross-section of this cell is shown in Figure 20. EDAX was performed on a similar section with the results presented in Table V. No interdiffusion of the component materials is detected within the sensitivity and resolution of the technique.

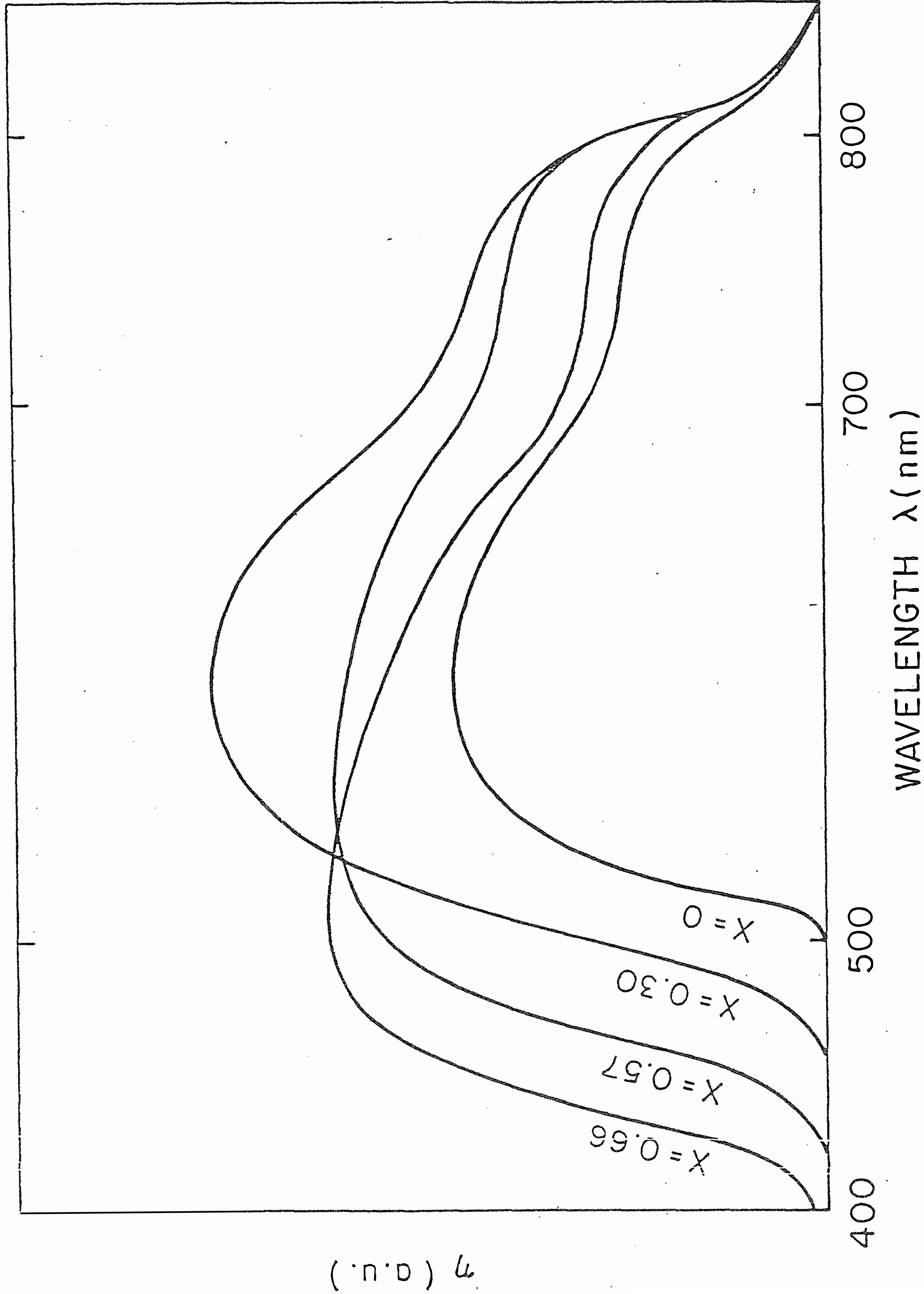

Figure 18. Collection Efficiencies As a Function of Wavelength for $(CdZn)S/Zn_3P_2$ Devices with Various Zinc Content

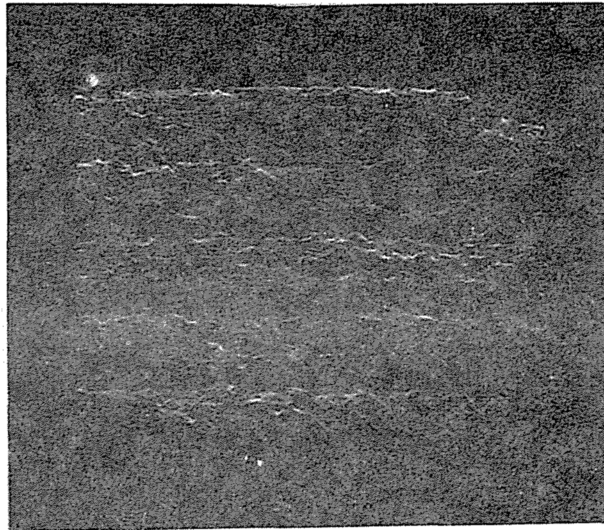

Figure 19. Scanning Laser Response of $Cd_{.62}Zn_{.38}S/Zn_3P_2$ Device #1791-1

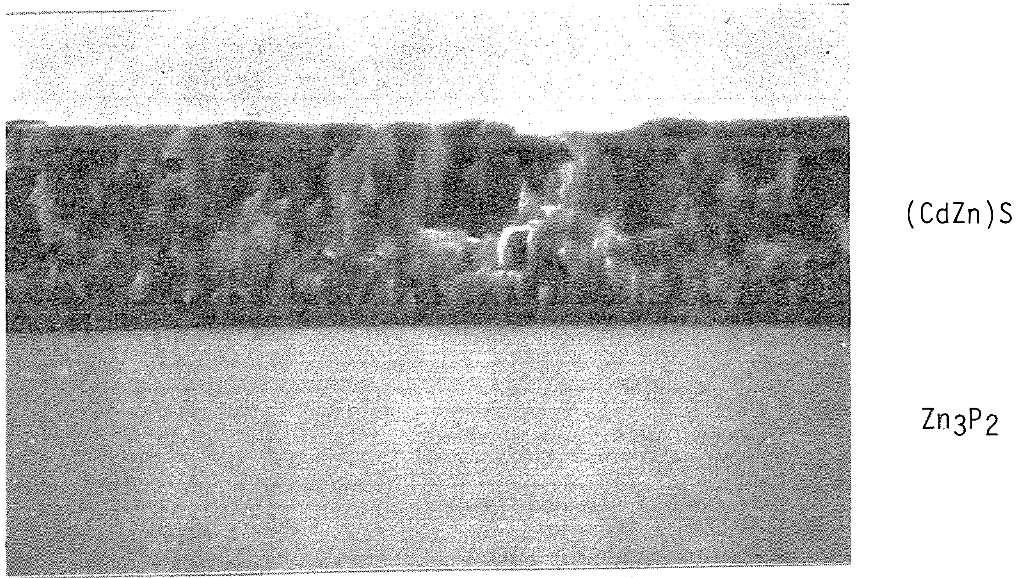

Figure 20. Back Scattered Electron Image in the Composition Mode for $(CdZn)S/Zn_3P_2$ Device #1791-6 - x 3,500

TABLE V

X-ray emission intensities on cross-section of 1791-6

Sampled area ~ 1 x 1 μm^2

Distance from the metallurgical junction (μm)	ZnKα	PKα	CdLα	SKα
3	1331	3102	-	
1	1226	3112	-	
0	625	1357	2604	3101
3	300	-	2854	3639

The existence of a sharp heterojunction was confirmed by an EBIC scan of a similar sample, 1792-1 conducted at SERI by R. Matson and shown in Figure 21.

C^{-2} vs voltage measurements were carried out as a function of frequency with the results shown in Table VI.

TABLE VI

Capacitance-voltage results as a function of frequency in the dark

$(CdZn)S/Zn_3P_2$ sample #1791-1

Frequency (H_Z)	ϕ_B(eV)	$d(C^{-2})/dV$ (cm^4/nF^2V)
0.1	0.324	$6.54.10^{13}$
1.0	0.338	$9.95.10^{13}$
4.0	0.782	$6.29.10^{13}$
10.0	Non linear behavior	

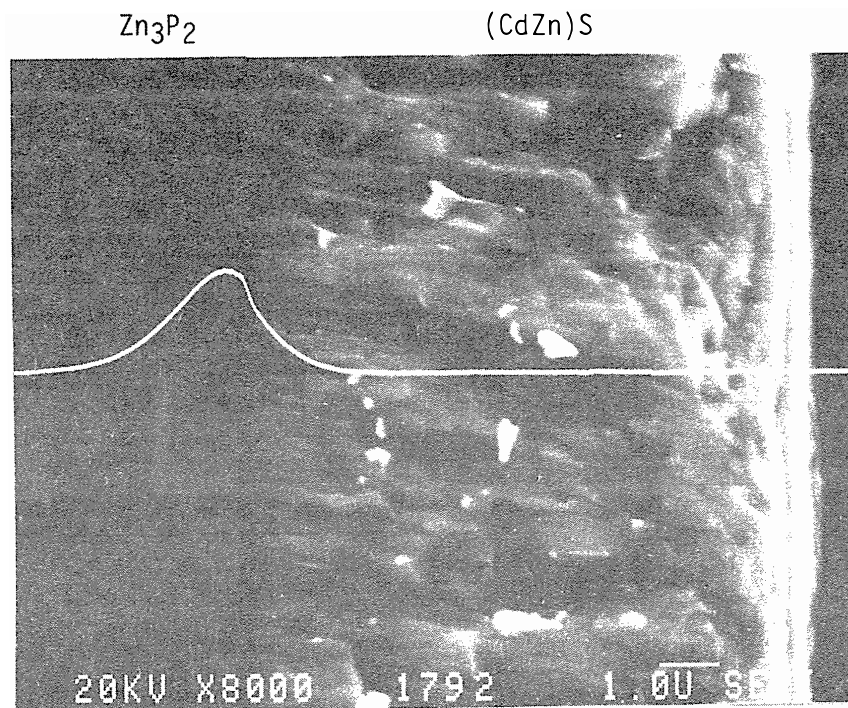

Figure 21. EBIC Response for $Cd_{.6}Zn_{.4}S/Zn_3P_2$
Device #1792-1
Courtesy R. Matson, SERI

The intercept increase with increasing frequency is interpreted to be due to the presence of interface states.

A range of surface pre-treatments and modifications to the junction structure were made in an attempt to improve the junction quality. (CdZn)S films were deposited at 125°C rather than 200°C and in other runs the Zn_3P_2 wafers were either pre-heated in hydrogen or thermally etched in the (CdZn)S deposition system prior to growth of the n-layer. Device properties resulting from these procedures showed scattered values but no consistent overall improvement in J_{SC}. As ZnS should be better matched to the Zn_3P_2, devices were made with thin interlayers of ZnS between Zn_3P_2 and a (CdZn)S layer containing 27% Zinc (Pure ZnS is too resistive to use for the entire n-layer). Run #1877 was deposited on 1500Å of ZnS and a cell from this run showed a V_{OC} of 0.49 V which is significantly higher than would be expected for the zinc content in the main n-layer (Figure 12 ~ 0.3 V) but the currents were very low.

Samples were heated in argon at temperatures ranging from 150°C to 350°C. The V_{OC} and J_{SC} of CdS/Zn_3P_2 devices improved by 10% after heating at 150°C but at higher temperatures no further improvement was observed. In $Cd_{1-x}Zn_xS/Zn_3P_2$ devices, the device series resistance increased and the J_{SC} decreased due to an increase in the resistivity of the (CdZn)S film.

Similar results were noted for the bulk and thin-film devices. In both cases the V_{OC} increases with x as predicted from theoretical considerations but the J_{SC} is lower than 20 mA/cm^2 expected for a Zn_3P_2 absorber.

A sequence of low temperature heat treatments were carried out on cells in the #1800 series, deposited on 500Å of ZnS, in an attempt to avoid the decline in cell performance resulting from heat treatments above ~ 200°C.

At the time of writing one sample had shown an increase in V_{oc} from 0.42 to 0.49 V and in J_{sc} from 0.61 to 1.22 mA/cm^2. A total heat treatment of 1480 hours at temperatures between 100 and 175°C had taken place. The cells will be further treated until the performance starts to decline.

6. Future Research

An initial boost to the development of devices based on Zn_3P_2 was provided by the relative ease with which good single crystals could be made. Using these crystals it was shown that the dominant acceptor is a phosphorus interstitial and that conductivity could be controlled by appropriate annealing in zinc or phosphorous atmospheres. It was also found that conductivity could be controlled using silver as an intentional dopant. In addition to these measurements, the optical absorption behavior was also extensively studied.

The good carrier properties readily available in bulk crystals and thin-films deposited by close spaced vapor transport, made it possible to develop quite efficient Schottky and Schottky grid devices. With this device structure, the good properties of the available Zn_3P_2 could be translated into good device behavior as there was little scope for deleterious effects as the devices were made. Arising out of the work on Schottkies it was found that Mg acted as a donor in Zn_3P_2 producing a quite efficient homojunction. However, it was also learned that Mg diffuses rapidly in Zn_3P_2 at room temperature thus rendering the homojunctions unstable. During the final years of this research effort, attention was focussed on heterojunctions as these were seen as the most plausible device to form the basis of a commercial cell. During these research efforts, it became increasingly evident that systematic further progress required a much more extensive knowledge of the basic chemical and electronic properties of Zn_3P_2 and in addition more choice and control of n type window materials would substantially assist in development of Zn_3P_2 heterojunctions.

The broad range of II-V compounds known to be semiconductors and the

extensive occurrence of solid solutions in this series justify extensive fundamental studies of this class of compounds. If such a research effort was carried out, it is quite certain that further developmental efforts on Zn_3P_2 solar cells would benefit significantly. There is also a very high probability that other potential solar cell materials would be identified and also that materials suitable for other types of devices would also be discovered. In the specific case of Zn_3P_2 heterojunctions, the foundation for future systematic cell development will be provided by a broad fundamental study of the material properties of Zn_3P_2 and the relation between material production and properties.

7. REFERENCES

1. Institute of Energy Conversion, University of Delaware, Annual Report on DOE/SERI Subcontract #XE-2-02048-1, May 1983

2. D. L. Kirk and M. S. Raven, Journal of Physics D, 9, 2015 (1976)

3. Institute of Energy Conversion, University of Delaware, 5th Quarterly Progress Report on DOE/SERI Subcontract #XR-9-8062-1, 1979

4. V. D. Vankar, S. R. Das, Prem Nath and K. L. Chopra, Phys. Sta. Sol.(a), 45, 665, (1978)

5. R. Bannaceur, R. B. Hall and R. B. Rothwarf, Proc. 3rd E. C. Photovoltaic Solar Energy Conference, Cannes, 1980

6. A. Catalano, J. Crystal Growth, 49, 681, (1980)

7. A. Catalano, M. Bhushan and N. Convers Wyeth, Proc. 14th IEEE Photovoltaic Specialists Conference, San Diego, p 641, (1980)

APPENDIX

INSTITUTE OF ENERGY CONVERSION

Publications On Zn_3P_2

1. A. Catalano, V. L. Dalal, E. A. Fagen, R. B. Hall, J. V. Masi, J. D. Meakin, G. Warfield and A. M. Barnett, "Zn_3P_2 As a Photovoltaic Material," First E.C. Photovoltaic Solar Energy Conference, 1977, (Reidel, Dordrecht, Holland, 1978) p. 644.

2. A. Catalano, V. L. Dalal, W. E. Devaney, E. A. Fagen, R. B. Hall, J. V. Masi and G. Warfield, "Zn_3P_2: A Promising Photovoltaic Material," Proceedings of the 13th IEEE Photovoltaic Specialists Conference, p. 288 (1978).

3. N. Convers Wyeth and A. Catalano, "Spectral Response Measurements of Minority Carrier Diffusion Length in Zn_3P_2," J. Appl. Phys., 50, 1403 (1979).

4. A. Catalano, J. V. Masi and N. Convers Wyeth, "Schottky Barrier Grid Devices on Zn_3P_2," Second E.C. Photovoltaic Solar Energy Conference, 1979, (Reidel, Dordrecht, Holland, 1979) p. 440.

5. A. Catalano and R. B. Hall, "Defect Dominated Conductivity in Zn_3P_2," J. Phys. Chem. Sol., 41, 635 (1980).

6. A. Catalano, "Growth of Large Zn_3P_2 Crystals," J. Crystal Growth, 49, 681 (1980).

7. N. Convers Wyeth and A. Catalano "Barrier Height of Evaporated Metal Contacts to Zn_3P_2," J. Appl. Phys., 51, 2286 (1980).

8. A. Catalano and M. Bhushan, "Evidence of p/n Homojunction Formation in Zn_3P_2," Appl. Phys. Letters, 37, 657 (1980).

9. A. Catalano, M. Bhushan and N. Convers Wyeth, "Thin Polycrystalline Films for Photovoltaic Solar Cells," Proceedings of the 14th IEEE Photovoltaic Specialists Conference, p. 641 (1980).

10. A. Catalano and M. Bhushan, "Zn_3P_2 Homojunction Devices", Presented at the First International Symposium on the Physics and Chemistry of II-V Compounds, Mogilany, Poland, September 1980.

11. A. Catalano and R. B. Hall, "Evidence of Defect Dominated Conductivity in Zn_3P_2," 9th International Symposium on the Reactivity of Solids, Cracow, Poland, September 1980.

12. M. Bhushan and A. Catalano, "Polycrystalline Zn_3P_2 Schottky Barrier Solar Cells," Appl. Phys. Lett., 38, 39 (1981).

13. L. L. Kazmerski, P. J. Ireland and A. Catalano, "Surface and Interface Properties of Zn_3P_2," Journ. of Vac. Sci. & Tech., 18, 368 (1981).

14. L. L. Kazmerski, P. J. Ireland and A. Catalano, "Interface Reactions in Mg/Zn_3P_2 Solar Cells," 15th IEEE Photovoltaic Specialists Conference Proceedings, p. 1083 (1981).

15. M. Bhushan and A. Catalano, "Zinc Phosphide Thin-Film Solar Cells," 15th IEEE Photovoltaic Specialists Conference, p. 1261 (1981).

16. P. S. Nayar and A. Catalano, "Zinc Phosphide-Zinc Oxide Heterojunction Solar Cells," Appl. Phys. Lett., 39, 105 (1981).

17. A. Catalano, "Photoluminescence and Optical Absorption of Mg_3P_2," Thin Solid Films, 83, L-141 (1981).

18. M. Bhushan, "Mg Diffused Zinc Phosphide n/p Junctions," J. Appl. Phys., 53, 514 (1982).

19. P. S. Nayar, "Properties of Zinc Phosphide/Zinc Oxide Heterojunctions," J. Appl. Phys., 53, 1069 (1982).

20. E. A. Fagen, "Optical Properties of Zn_3P_2," J. Appl. Phys., 50, 6505 (1979).

21. M. Bhushan, "Schottky Solar Cells on Thin Polycrystalline Zn_3P_2 Films," Appl. Phys. Lett., 40, 51 (1982).

22. J. M. Pawlikowski, "Comments on Zn_3P_2 Band Structure," J. Appl. Phys., 53, 3639 (1982).

23. J. M. Pawlikowski, "Absorption Edge of Zn_3P_2," Phys. Review (b), 26, 4711 (1982).

24. M. Bhushan, "Zn_3P_2 Thin-Film Solar Cells," Fourth E.C. Photovoltaic Solar Energy Conference, 1982, (Reidel, Dordrecht, Holland, 1982) p. 844.

25. M. Bhushan, J. M. Pawlikowski, I. Pereyra, "Zinc Phosphide for Solar Cell Applications," Proc. Electrochem. Soc. 82, 505 (1982).

CONTRACT PROGRESS REPORTS

AGENCY	CONTRACT NUMBER	REPORT	
ERDA	E(49-18)-2460	Quarterly Progress Report	7/1/76 - 9/30/76
ERDA	E(49-18)-2460	Quarterly Progress Report	10/1/76 - 12/31/76
ERDA	E(49-18)-2460	Quarterly Progress Report	1/1/77 - 3/31/77
ERDA	E(49-18)-2460	Quarterly Progress Report	4/1/77 - 6/30/77
DOE	EX-76-C-01-2460 [Formerly E(49-18)-2460]	Quarterly Progress Report	7/1/77 - 9/30/77
DOE	EX-76-C-01-2460 [Formerly E(49-18)-2460]	Quarterly Progress Report	10/1/77 - 12/31/77
DOE	EX-76-C-01-2460 [Formerly E(49-18)-2460]	Quarterly Progress Report	1/1/78 - 3/31/78
DOE	EX-76-C-01-2460 [Formerly E(49-18)-2460]	Quarterly Progress Report	4/1/78 - 6/30/78
DOE	EX-76-C-01=2460 [Formerly E(49-18)-2460]	Quarterly Progress Report	7/1/78 - 9/1/78
DOE	EX-76-C-01-2460 [Formerly E(49-18)-2460]	Final Progress Report	7/1/76 - 9/1/78
SERI	XR-9-8062-1	Quarterly Progress Report	9/1/78 - 11/30/78
SERI	XR-9-8062-1	Quarterly Progress Report	12/1/78 - 2/28/79
SERI	XR-9-8062-1	Quarterly Progress Report	3/1/79 - 5/31/79
SERI	XR-9-8062-1	Quarterly Progress Report	6/1/79 - 8/31/79
SERI	XR-9-8062-1	Quarterly Progress Report	9/1/79 - 12/1/79
SERI	XR-9-8062-1	Quarterly Progress Report	12/1/79 - 2/29/80
SERI	XR-9-8062-1	Quarterly Progress Report	3/1/80 - 5/31/80
SERI	XR-9-8062-1	Quarterly Progress Report	6/1/80 - 8/31/80

SERI	XR-9-8062-1	Quarterly Progress Report	9/1/80 - 11/30/80
SERI	XR-9-8062-1	Quarterly Progress Report	12/1/80 - 2/28/81
SERI	XR-9-8062-1	Quarterly Progress Report	3/1/81 - 5/31/81
SERI	XR-9-8062-1	Quarterly Progress Report	6/1/81 - 8/31/81
SERI	XR-9-8062-1	Quarterly Progress Report	9/1/81 - 11/30/81
SERI	XR-9-8062-1	Final Progress Report	9/1/78 - 3/31/82
SERI	XE-2-02048-1	Quarterly Progress Report	3/1/82 - 5/31/82
SERI	XE-2-02048-1	Semi-Annual Progress Report	4/1/82 - 9/30/82
SERI	XE-2-02048-1	Annual Progress Report	4/1/82 - 3/31/83
SERI	XE-2-02048-1	Quarterly Progress Report	4/1/83 - 6/30/83
SERI	XE-2-02048-1	Semi-Annual Progress Report	4/1/83 - 9/30/83

Document Control Page	1. SERI Report No. SERI/STR-211-2515	2. NTIS Accession No.	3. Recipient's Accession No.

4. Title and Subtitle

Zn_3P_2 as an Improved Semiconductor for Photovoltaic Solar Cells

5. Publication Date

March 1985

6.

7. Author(s)

M. Bhushan, J. D. Meakin

8. Performing Organization Rept. No.

9. Performing Organization Name and Address

Institute of Energy Conversion
University of Delaware
Newark, DE 19716

10. Project/Task/Work Unit No.

3433.10

11. Contract (C) or Grant (G) No.

(C) XE-2-02048-1

(G)

12. Sponsoring Organization Name and Address

Solar Energy Research Institute
1617 Cole Boulevard
Golden, Colorado 80401

13. Type of Report & Period Covered

Technical Report

14.

15. Supplementary Notes

Technical Monitor: Rick Mitchell

16. Abstract (Limit: 200 words)

Development efforts have been made on two heterojunctions with Zn_3P_2; namely, Zn_3P_2/ZnSe and An_3P_2/(CdZn)S. In both cases, improved open-circuit voltages were achieved, but control of the material properties of the heterojunction partner has limited short-circuit currents and overall efficiency. In the case of ZnSe, the high resistivities of deposited thin-films were efficiency-limiting on all devices. In the case of (CdZn)S, it is concluded that high interface recombination rates are controlling the short-circuit current and limiting the overall efficiency. A more fundamental study of the Zn_3P_2/(CdAn)S heterojunction will be necessary in order to make further optimization of this device possible.

17. Document Analysis

a. Descriptors Doped Materials ; Efficiency ; Electric Conductivity ; Solar Cells ; Zinc Phosphides ; Zinc Selenides

b. Identifiers/Open-Ended Terms

c. UC Categories

63

18. Availability Statement

National Technical Information Service
U.S. Department of Commerce
5285 Port Royal Road
Springfield, Virginia 22161

19. No. of Pages

59

20. Price

A04

Form No. 0069 (3-25-82)